Available online at www.sciencedirect.com
SCIENCE DIRECT
Precambrian Research 145 (2006) 53–80
Precambrian Research
www.elsevier.com/locate/precamres

U–Pb geochronology of the MacQuoid supracrustal belt and Cross Bay plutonic complex: Key components of the northwestern Hearne subdomain, western Churchill Province, Nunavut, Canada

William J. Davis *, Simon Hanmer, Subhas Tella, Hamish A. Sandeman, James J. Ryan

Geological Survey of Canada, 601 Booth Street, Ottawa, Ont., Canada K1A 0E8

Received 26 January 2005; received in revised form 4 November 2005; accepted 17 November 2005

Abstract

New geological and geochronological data from the MacQuoid supracrustal belt and the geometrically overlying Cross Bay plutonic complex highlight a distinct tectonothermal evolution for the northwestern part of the Hearne domain (northwestern Hearne subdomain), compared with adjacent areas in the Rae and Hearne, of the western Churchill Province, Canada. The supracrustal and intrusive rocks dominantly formed in the Neoarchean between <2.74 and 2.65 Ga, with minor 2.61 Ga granite, and experienced a polycyclic Neoarchean and Paleoproterozoic deformational history. The dominant tectonic fabric throughout much of the area formed between 2.56 and 2.50 Ga, including the Big Lake shear zone, a granulite-facies mylonite zone that juxtaposed the Cross Bay plutonic complex over the MacQuoid supracrustal belt at 2.50 Ga. The fabric transposed earlier fabrics whose age is poorly constrained. Additional tectonic events occurred during the Paleoproterozoic at 1.90 Ga, and 1.84–1.81 Ga. Differences between the geological histories of the northwestern part of the Hearne domain relative to the immediately adjacent Rae and Hearne areas highlight the tectonically distinct character of the northwestern Hearne subdomain.

Keywords: Geochronology; Western Churchill; Rae; Hearne; Tectonic evolution

1. Introduction

The western Churchill Province is one of the largest, yet poorly known fragments of Archean crust in the world (Fig. 1A). The area is composed of variably reworked Archean rocks, with minor Paleoproterozoic plutons and cover sequences, and is flanked to the northwest and southeast by the ∼2.0–1.9 Ga Taltson-Thelon and ∼1.9–1.8 Ga Trans-Hudson orogens, respectively. Hoffman (1988) separated the region into the Rae and Hearne provinces along the trace of the Snowbird tectonic zone, a northeast-trending geophysically defined feature (Gibb et al., 1983; Thomas and Gibb, 1985). The designation of the Rae and Hearne at province status hinges on the interpretation that the Snowbird zone represented a fundamental suture in the Paleoproterozoic, separating Archean provinces with distinct histories. This remains a subject of some debate. With the exception of exposures in northern Saskatchewan, the geological nature and expression of the Snowbird zone and its flanking areas is poorly known and its significance has remained speculative and controversial (Hanmer et al., 1995; Ross, 2002; Mahan et al., 2003). This ambiguity reflects the lack of baseline geological data, calibrated using modern geochronological methods, required to compare the timing of crust formation and subsequent

* Corresponding author. Tel.: +1 613 943 8780.
E-mail address: bidavis@nrcan.gc.ca (W.J. Davis).

0301-9268/$ – see front matter © 2005 Elsevier B.V. All rights reserved.
doi:10.1016/j.precamres.2005.11.016

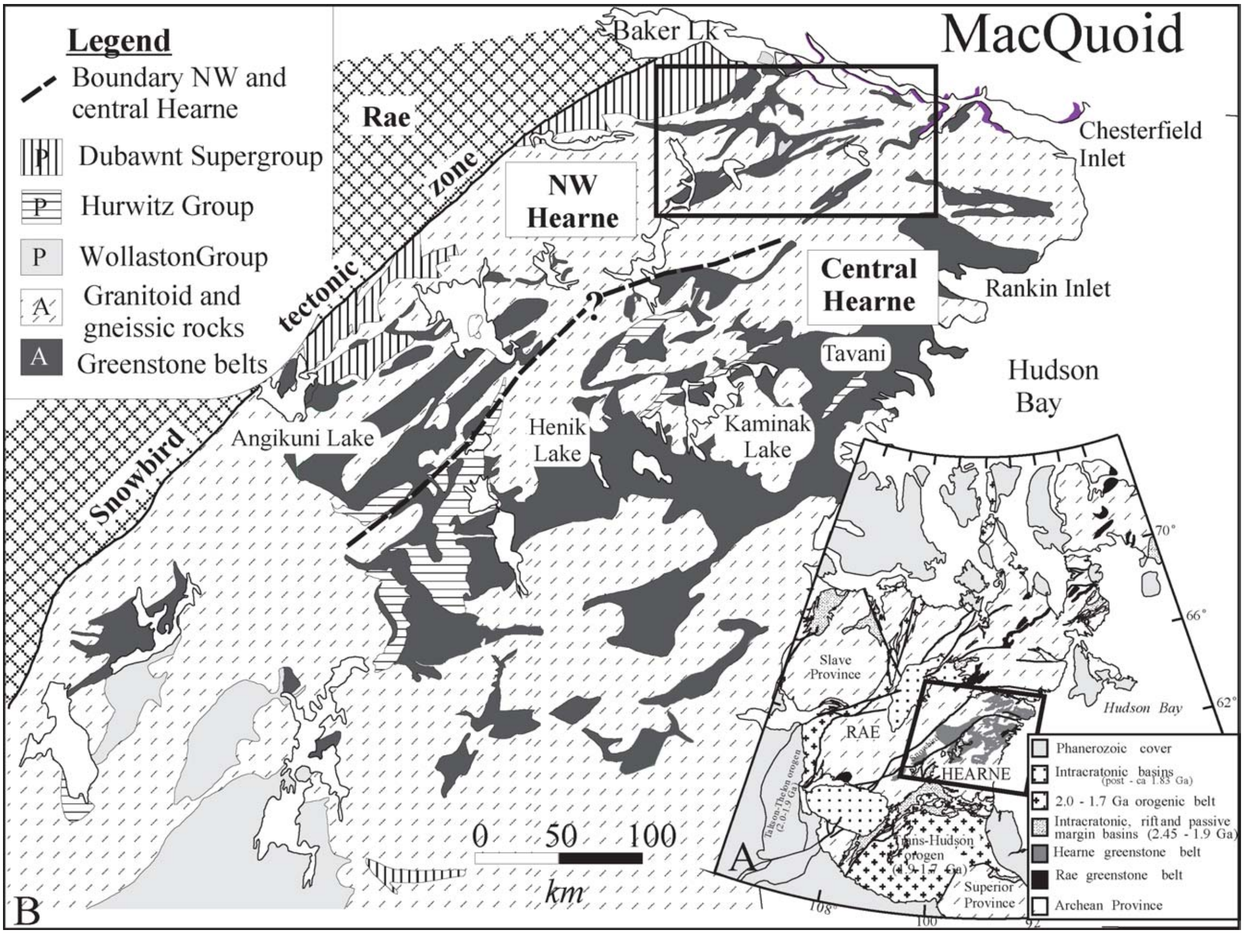

Fig. 1. (A) Major tectonic components of the exposed western Canadian Shield. The area of the western Churchill Province is divided into Rae and Hearne domains by the Snowbird tectonic zone (STZ). WLG, Woodburn Lake group; PAG, Prince Alberta Group. Box indicates the area shown in B. (B) Distribution of supracrustal belts within the Hearne domain. Dashed line approximate boundary between northwestern and Central Hearne subdomains. Box contains location of Fig. 2.

deformation in various parts of the Rae and Hearne. In this paper new geological and geochronological data are presented for the MacQuoid–Gibson Lakes area in the northwestern part of the Hearne domain (Fig. 1B) adjacent to the Chesterfield segment of the Snowbird tectonic zone. The data address the timing of the principal crust-forming and tectono-thermal events in the area, and are used to examine the geological history of this area in the broader tectonic context of the Rae and Hearne during the Neoarchean.

2. Regional geological setting

The Archean component of the Rae (Fig. 1A) is characterized, in part by, extensive, Neoarchean, komatiite-bearing volcanic belts with stratigraphically overlying quartzites, and metasediemtary belts. The sequences were deposited on extended continental crust containing locally identified Mesoarchean basement (Zaleski et al., 2001). Granite plutons intruded over a wide area of the Rae between 2.62 and 2.58 Ga (LeCheminant and Roddick, 1991). Although dominated by Archean crustal ages, the predominant regional tectonothermal structures developed at or after 2.35 Ga, and ∼1.85–1.81 Ga, the latter associated with widespread granite plutonism (Carson et al., 2004; Zaleski et al., 2001). In contrast, Archean components of the Hearne domain, northeast of the Athabasca Basin (Fig. 1B), include Neoarchean mafic to felsic volcanic and plutonic rocks that, with a few exceptions proximal to the trace of the Snowbird tectonic zone, do not indicate interaction with Mesoarchean basement (Aspler et al., 1999; Cousens et al., 2004; Sandeman et al., 2004a,b, 2006). Until recently, the volcanic rocks of the Rae domain

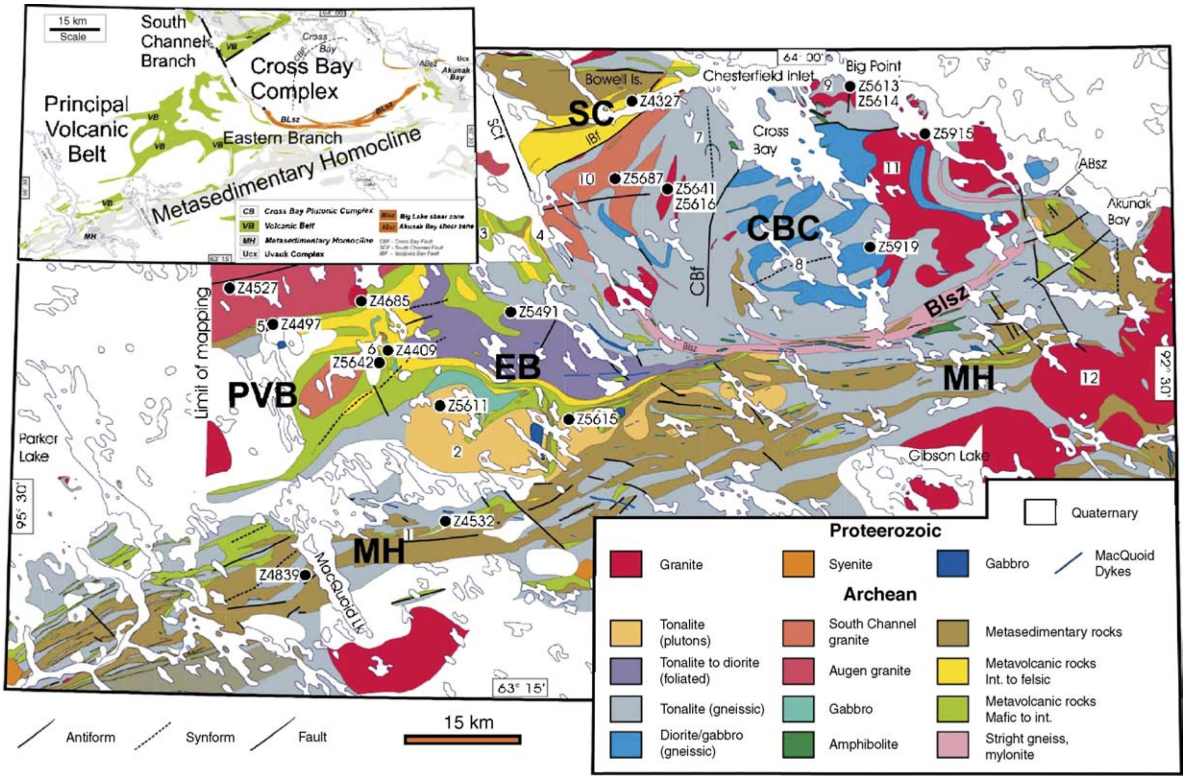

Fig. 2. Geology of the MacQuoid supracrustal belt, after Tella et al. (2001). Inset shows principal subdomains referred to in text: CBC, Cross Bay plutonic complex; PVB, principal volcanic belt; EB, eastern branch of PVB; SC, South Channel volcanic branch; MH, metasedimentary homocline. Other abbreviations: Absz, Akunak Bay shear zone; BLsz, Big Lake shear zone; CBF, Cross Bay fault; IbF, Ippijuaq Bay fault; SCF, South Channel fault. Geochronological sample locations and numbers are indicated. Other numbers correspond to locations referred to in the text.

were thought to be ~100 m.y. older than those of the Hearne (Schau et al., 1978; Frisch, 1982; Tella et al., 1985; Henderson et al., 1991; Roddick et al., 1992). However, they are now known to only slightly predate (~2740–2710 Ma) supracrustal belts in the Hearne (Fig. 2; ~2710–2680 Ma; Davis et al., 2000, 2004).

Supracrustal belts within the Hearne have been considered together as part of the Rankin-Ennadai greenstone belt (e.g. Aspler and Chiarenzelli, 1996). However, important regional differences have been identified (Davis et al., 2000). The central part of the Hearne is composed of Neoarchean supracrustal and associated plutonic rocks that developed over a short time interval between 2710 and 2680 Ma (Davis et al., 2004). Regional greenschist-facies metamorphism and deformation occurred at ~2680 Ma, and this area remained thermotectonically quiescent until ~1830 Ma (Berman et al., 2002b; Hanmer et al., 2004; Davis et al., 2004). In contrast, areas in the northwestern part of the Hearne (Yathkyed, Angikuni and MacQuoid supracrustal belts; Fig. 1B) preserve a more complex, poly-metamorphic history with variably developed amphibolite-facies metamorphism and deformation at ~2.66–2.64, ~2.55–2.50, 1.90 and 1.84–1.81 Ga (Berman et al., 2000, 2002a,b; Stern and Berman, 2001; MacLachlan et al., 2005a,b; Aspler et al., 1999; Hanmer et al., 2006). Additional geological elements that distinguish the northwestern from the central Hearne include the occurrence of ~2.60 Ga granite plutons, and distinct generations of mafic dyke swarms (Davis et al., 2000). The entire area was affected by ~1.83–1.81 Ga deformation, plutonism and metamorphism as a consequence of convergence of the Trans-Hudson and Paleoproterozoic collisions on the western edge of Laurentia (Ross, 2002).

3. Geology of the MacQuoid belt

The MacQuoid–Gibson Lake area (Fig. 2; Tella et al., 2001; Hanmer et al., 2006; Sandeman et al., 2000b, 2006; Stern and Berman, 2001; Ryan et al., 2000), is divided into two geological subdomains: the MacQuoid supracrustal belt, comprising the principal volcanic belt and the metasedimentary homocline, and the Cross Bay plutonic complex (CBC; Hanmer et al., 2006, Fig. 2). The Big Lake shear zone (BLsz, Fig. 2), a granulite-facies mylonite zone, separates the subdomains and is interpreted as a ∼2.5 Ga thrust fault that placed the CBC over the supracrustal belt (Ryan et al., 2000).

4. MacQuoid supracrustal belt

The MacQuoid supracrustal belt comprises a moderately north-dipping, predominantly metasedimentary homocline with extensive sheets of gneissic tonalite, and overlying predominantly volcanic belts intruded by tonalitic plutons. The volcanic belts occur in a number of geographically discrete areas, however, transposition by later deformation, described further below, has obscured the primary relationships between the different volcanic and sedimentary belts. The area is intruded by multiple generations of Neoarchean and Paleoproterozoic plutonic rocks, and by the widespread, east-trending MacQuoid mafic dyke swarm (∼2.19 Ga; Tella et al., 1997b).

4.1. Metasedimentary homocline

The metasedimentary homocline (MH, Fig. 2) is composed of moderately north–northwest-dipping (average 40–50Circ), concordant panels of biotite ± garnet-bearing metasedimentary rocks, with subordinate, mafic metavolcanic rocks (amphibolite), gneissic tonalite and tonalitic plutons (Tella et al., 1997b; Hanmer et al., 1999a). The igneous rocks have juvenile Nd isotopic compositions (Sandeman et al., 2006). Tonalite gneisses and plutons form intrusive sheets and discrete bodies within the supracrustal panel and constitute ∼50% of the homocline by volume. Two types of gneissic tonalite are identified. The first type contains a gneissosity derived from closely packed, mafic xenoliths of fine-grained, homogeneous amphibolite (Fig. 3). The second type has a gneissosity defined by thin (5–10 cm), pink granitoid veins, oriented along the regional foliation in the host tonalite (Fig. 4). The discrete tonalite to granodiorite plutons are leucocratic and foliated, but locally preserve an igneous texture.

4.2. Volcanic belts

Two geographically defined volcanic belts are identified. The principal volcanic belt (PVB, Fig. 2) forms an open, map-scale, concave-east, arcuate structure that overlies the homocline, and includes a laterally extensive, moderately north-dipping, eastern branch (EB, Fig. 2). The latter passes westwards into an area of regional-scale, upright, moderately east–northeast-plunging folds. The exact relationship of the PVB to the structurally underlying metasedimentary homocline is poorly known. The principal volcanic belt is com-

Fig. 3. Tonalitic gneiss derived from intrusive tonalite with abundant, closely packed, and disrupted mafic xenoliths and panels of fine-grained, well layered to homogenous amphibolite.

Fig. 4. Tonalitic gneiss derived from tonalite riddled with long, narrow (5–10 cm) pink granitoid veins, emplaced along the regional foliation.

positionally zoned, with predominantly mafic volcanic rocks and subvolcanic gabbro in the south, and intermediate volcanic rocks in the north. The mafic rocks are fine-grained, massive to layered (1–5 cm), hornblende-garnet ± clinopyroxene amphibolites, with rare, relict pillow structures. Intermediate volcanic rocks are fine-grained and homogeneous, with local crystal and lapilli tuffs.

A discontinuous belt of northeast-trending, fine-grained, garnet amphibolite and associated intermediate to felsic volcanic and sedimentary rocks extends from the PVB towards Chesterfield Inlet. The primary relationship of these volcanic rocks to those in the PVB is not known. The northern volcanic belt is flanked to the north by an east-trending panel of uniform semipelitic rocks with widespread garnet-sillimanite-kyanite, and pervasive, quartzo-feldspathic, metamorphic segregations (Bowell Island, Fig. 2). These metasedimentary rocks cannot be directly linked to those in the homocline and may represent an independent package intercalated with the intermediate volcanic rocks of South Channel.

Three isolated occurrences of conglomerate occur within the volcanic belts: (i) quartz pebble conglomerate with interbedded arenite and quartzite; (ii) polymictic conglomerate with foliated tonalite, quartz and minor volcanic clasts and (iii) volcanic breccia and conglomerate with subordinate quartz, quartz arenite and carbonate clasts (#4–6, Fig. 2, respectively).

4.3. Intrusive rocks

Tonalite to granodiorite rocks similar to those within the metasedimentary homocline also intruded the volcanic belts. Most prominent are three large, lobate plutons (#2, Fig. 2) that underlie the eastern branch of the principal volcanic belt. The northern margin of the principal volcanic belt is flanked by a large, poorly exposed, augen granite pluton (north of #5, Fig. 2; Tella et al., 1997b).

The MacQuoid dykes, a swarm of 70–120° trending, subvertical, mafic sheets, 2–20 m thick, but locally up to 500 m, intruded the metasedimentary homocline, as well as the Cross Bay plutonic complex (Fig. 2; Hanmer et al., 1999a,b). Tella et al. (2001) reported an age of ∼2.19 Ga for one of the dykes, and correlated them with the ∼2.19 Ga Tulemalu mafic dyke swarm in the Angikuni–Yathkyed area of the northwestern Hearne subdomain (Fig. 2; Eade, 1986; Fahrig et al., 1984; Tella et al., 1997a; LeCheminant et al., 1997). The dykes are coarse grained, locally plagioclase-phyric, and commonly preserve chilled margins. Garnet-clinopyroxene coronae around plagioclase are locally developed that yield metamorphic P-T estimates of ∼700–800 °C at ∼1.0–1.2 GPa and dated at ∼1.90 Ga (Berman et al., 2000). In the MacQuoid supracrustal belt, the dykes are generally non-foliated and locally cross-cut the regional transposition fabric in the host rock.

Proterozoic granites intruded in a number of areas, particularly along the southern and eastern parts of the MacQuoid belt. They are composed of biotite ± fluorite monzogranite, and are interpreted to be part of a granite province that developed over a wide area of the western Churchill Province at ∼1830 Ma (Tella et al., 2000, 2001; Peterson et al., 2000, 2002; van Breemen et al., 2005). A sample of granite from the eastern part of the area has been dated at 1842 ± 5.4 Ma (van Breemen et al., 2005).

4.4. Structure of the MacQuoid supracrustal belt

Deformation fabrics in the eastern part of the metasedimentary homocline and the eastern branch of the principal volcanic belt are dominated by a single, moderately (40–50°) north–northwest-dipping, layer-parallel, penetrative foliation, and a moderately to steeply pitching, north to northeast-plunging extension lineation. The latter is well developed in the eastern branch of the principal volcanic belt (Hanmer et al., 1999b). The single fabric was derived by progressive transposition of earlier fabrics that are locally preserved in the western part of the belt (see Ryan et al., 1999 and Hanmer et al., 2006). Ryan et al. (1999, 2000) demonstrated that the regional transposition fabric and earlier structures were deformed about upright, moderately east–northeast-plunging folds which they interpreted as Paleoproterozoic in age.

The gneissic tonalite sheets in the metasedimentary homocline contain the regional transposition fabric. The transposition fabric observed in the volcanic rocks is recorded in the marginal zones of these plutons, and wraps around them (Fig. 2), indicating that it post-dates the emplacement of the plutons.

5. U–Pb geochronology of the MacQuoid supracrustal belt

5.1. Analytical techniques

Heavy mineral concentrates were prepared by standard techniques (crushing, grinding, Wilfley™ table, heavy liquids), and sorted by magnetic susceptibility using a Frantz™ isodynamic separator. All zircon fractions and selected titanite fractions (Table 1) were air

Table 1
U–Pb ID-TIMS analytical data

Fraction	Description	Mag	# Grains	Wt. (μg)	U[2] (ppm)	Pb*[2] (ppm)	Pbc[1] (pg)	$^{206}Pb/^{204}Pb$ [1]	$^{208}Pb/^{206}Pb$ [2]	$^{207}Pb/^{235}U$ [2]	$\pm ^{207}Pb/^{235}U$	$^{206}Pb/^{238}U$ [2]	$\pm ^{206}Pb/^{238}U$	$^{207}Pb/^{206}Pb$ [2]	$\pm ^{207}Pb/^{206}Pb$	$^{206}Pb/^{238}U$	Apparent ages (Ma) $\pm ^{206}Pb/^{238}U$	Apparent ages (Ma) $^{207}Pb/^{235}U$	$\pm ^{207}Pb/^{235}U$	$^{207}Pb/^{206}Pb$	$\pm ^{207}Pb/^{206}Pb$	Disc. (%)
Z4409: FelsicVolcanic Rock (96-txv-078)																						
1	Z,pBr,tur,pr	NM1	1	3	136	81	3	1717.9	0.152	13.547	0.029	0.5172	0.0011	0.18997	0.00009	2687.2	9.4	2718.5	4.1	2741.9	1.5	2.4
2	Z,pBr,tur,pr	NM0	2	2	101	61	27	267.8	0.138	13.939	0.060	0.5332	0.0018	0.18961	0.00046	2754.8	15.0	2745.6	8.2	2738.8	7.9	−0.7
3	Z,pBr,tur,pr	NM0	2	4	64	38	5	1827.1	0.136	13.721	0.035	0.5250	0.0013	0.18957	0.00010	2720.1	11.3	2730.6	4.8	2738.4	1.7	0.8
4	Z,pBr,tur,pr	NM1	1	2	183	104	1	2266.7	0.114	13.206	0.024	0.5068	0.0009	0.18898	0.00009	2643.0	7.7	2694.5	3.4	2733.3	1.5	4.0
5	Z,pBr,tur,pr	NM1	1	1	240	139	4	1612.9	0.113	13.432	0.038	0.5193	0.0015	0.18760	0.00010	2696.2	12.5	2710.5	5.4	2721.2	1.7	1.1
Z5491: FelsicVolcanic Rock (98-TXJ-184)																						
1	Z,clr,co,sub,eq,res	Dia	9	4	116	69	24	705.9	0.154	13.036	0.021	0.5157	0.0005	0.18333	0.00019	2681.0	4.5	2682.3	3.1	2683.2	3.4	0.1
2	Z,clr,co,sub,pr,res	Dia	9	7	96	56	7	3120.2	0.149	12.939	0.016	0.5121	0.0005	0.18324	0.00009	2665.7	4.2	2675.2	2.3	2682.4	1.5	0.8
3	Z,clr,co,sub,pr,res	Dia	9	5	73	43	24	466	0.152	13.053	0.029	0.5168	0.0007	0.18319	0.00027	2685.4	5.9	2683.5	4.1	2682.0	4.9	−0.2
4	Z,clr,co,sub,pr,res	Dia	4	6	47	28	2	3781.9	0.146	12.984	0.017	0.5141	0.0006	0.18316	0.00010	2674.2	4.9	2678.5	2.5	2681.7	1.7	0.3
Z5642: FelsicVolcanic Rock (98-txj-109)																						
1	Z,clr,co,pr	M1	4	3	118	68	23	510.9	0.119	12.882	0.029	0.5091	0.0006	0.18350	0.00029	2652.9	5.3	2671.0	4.3	2684.8	5.3	1.5
2	Z,clr,co,pr	M1	6	3	117	70	4	2624.9	0.182	12.789	0.018	0.5103	0.0006	0.18177	0.00010	2657.8	5.2	2664.2	2.7	2669.1	1.8	0.5
3	Z,clr,co,st,pr	M3	1	2	118	69	3	2043.6	0.136	12.771	0.020	0.5121	0.0008	0.18086	0.00017	2665.7	7.0	2662.9	3.0	2660.7	3.2	−0.2
4	Z,clr,co,el,pr	M3	3	2	247	141	18	990.8	0.156	12.301	0.019	0.4948	0.0005	0.18033	0.00015	2591.2	4.7	2627.7	2.8	2655.9	2.8	3.0
5	Z,clr,co,pr	M3	3	2	156	92	2	4341.3	0.219	12.140	0.017	0.4907	0.0006	0.17944	0.00010	2573.6	5.1	2615.3	2.6	2647.7	1.8	3.4
6	Z,clr,co,pr	M3	5	4	154	82	3	6145.8	0.129	11.561	0.016	0.4755	0.0006	0.17636	0.00008	2507.4	4.9	2569.6	2.5	2618.9	1.6	5.1
Z4327: Dacite Breccia (HVA-k93-643)																						
1	Z,clr,co,eu,pr	NM0	4	7	102	58	8	2517.6	0.149	12.419	0.016	0.5014	0.0005	0.17965	0.00009	2619.6	4.5	2636.6	2.4	2649.7	1.6	1.4
2	Z,clr,co,pr	NM0	6	2	40	22	2	709	0.085	12.462	0.051	0.5070	0.0018	0.17827	0.00045	2643.7	15.7	2639.8	7.7	2636.8	8.3	−0.3
3	Z,clr,co,eu,pr	NM0	10	10	31	17	9	1049.8	0.097	12.125	0.031	0.4972	0.0012	0.17687	0.00015	2601.7	10.2	2614.1	4.8	2623.7	2.7	1.0
4	Z,clr,co,eu,pr	NM0	7	5	55	28	17	469.6	0.092	11.060	0.054	0.4678	0.0020	0.17146	0.00035	2474.1	17.8	2528.2	9.1	2572.0	6.9	4.6
5	Z,clr,co,pr	NM0	2	4	33	16	14	288	0.107	10.505	0.043	0.4606	0.0017	0.16540	0.00036	2442.4	14.8	2480.4	7.6	2511.7	7.3	3.3
6	Z,clr,co,eu,pr	NM0		6	90	42	5	3238	0.078	9.906	0.019	0.4422	0.0008	0.16248	0.00009	2360.4	7.1	2426.1	3.6	2481.7	1.8	5.8
7	Z,clr,co,eu,pr	NM0	6	5	59	28	5	1601.2	0.064	9.789	0.025	0.4442	0.0011	0.15984	0.00012	2369.3	9.9	2415.1	4.7	2454.0	2.6	4.1
8T	T,Br,clr,an	0.75A	11	88	90	31	159	1077.7	0.044	5.476	0.009	0.3415	0.0003	0.11630	0.00012	1893.8	3.0	1896.8	2.8	1900.1	3.7	0.4
9T	T,pBr,clr,an	0.75A	16	49	99	33	66	1587.5	0.031	5.478	0.008	0.3416	0.0003	0.11630	0.00009	1894.5	3.0	1897.2	2.4	1900.1	2.7	0.3
Z4497: Polymictic conglomerate (96-tx-088)																						
1	tur,pBr,pr,fg	Dia	1	3	140	119	25	640.8	0.125	27.545	0.049	0.6958	0.0010	0.28713	0.00024	3404.5	7.6	3403.0	3.5	3402.1	2.6	−0.1
2	clr,pY, eu,pr	Dia	1	4	106	85	4	3902.9	0.097	26.207	0.043	0.6703	0.0010	0.28354	0.00012	3307.2	7.7	3354.3	3.2	3382.5	1.4	2.9
3	clr,pBr,ro,sub	Dia	1	7	46	36	1	4040.6	0.124	24.017	0.038	0.6590	0.0009	0.26433	0.00011	3263.2	7.4	3269.1	3.1	3272.7	1.3	0.4
4	clr,y,an,fg	Dia	1	16	110	88	9	7593.4	0.179	23.153	0.027	0.6415	0.0006	0.26176	0.00011	3194.9	4.7	3233.4	2.3	3257.3	1.3	2.4
5	clr,pBr,ro,sub	Dia	1	5	44	42	0	2318.7	0.456	22.799	0.050	0.6385	0.0013	0.25895	0.00012	3183.3	10.5	3218.4	4.2	3240.4	1.5	2.2
6	clr,y,an,fg	Dia	1	10	109	85	3	16220.5	0.254	19.903	0.024	0.6092	0.0006	0.23696	0.00010	3066.7	4.7	3086.7	2.3	3099.7	1.3	1.3
7	clr,pY, eu,pr	Dia	1	8	103	65	4	7044.7	0.099	15.956	0.020	0.5561	0.0006	0.20809	0.00009	2850.5	4.7	2874.1	2.4	2890.8	1.4	1.7
Z4532: Tonalite (96-tx-022)																						
1	Z,clr,pY,sub,pr	M0.5	1	2	101	58	2	2064.4	0.100	13.016	0.028	0.5165	0.0011	0.18277	0.00012	2684.2	9.0	2680.8	4.0	2678.2	2.1	−0.3
2	Z,clr,pY,sub,pr	M0.5	4	1	270	155	5	1676.5	0.117	12.887	0.023	0.5121	0.0008	0.18253	0.00010	2665.4	7.2	2671.4	3.4	2676.0	1.9	0.5
3	Z,tur,py,sub,pr,fr	M0.5	5	1	304	152	192	62.5	0.086	11.399	0.281	0.4598	0.0120	0.17980	0.00253	2438.7	105.6	2556.3	46.1	2651.0	45.9	9.6
4	Z,tur, eq,pr	M0.5	6	3	122	65	39	232.4	0.102	11.949	0.065	0.4823	0.0027	0.17967	0.00054	2537.4	23.8	2600.4	10.2	2649.9	10.0	5.1
5	Z,clr,pY,sub,pr	M0.5	5	1	526	281	13	1249.9	0.078	12.127	0.019	0.4952	0.0006	0.17760	0.00012	2593.3	5.2	2614.3	2.9	2630.6	2.2	1.7
6T	T,clr,Br,fg	0.75A	16	35	300	140	647	458	0.068	9.618	0.023	0.4404	0.0004	0.15838	0.00029	2352.5	3.8	2398.9	4.3	2438.5	6.2	4.2
7T	T,clr,co,fg,fr	0.75A	20	21	376	151	81	2477.8	0.022	8.465	0.009	0.3971	0.0003	0.15459	0.00006	2155.8	3.1	2282.1	1.9	2397.4	1.4	11.8
8T	T,clr,co,fg,fr	0.75A	20	26	138	55	56	1634.9	0.017	8.313	0.010	0.3966	0.0004	0.15204	0.00008	2153.1	3.4	2265.8	2.1	2369.1	1.9	10.7
9T	T,clr,pBr,fg	0.75A	20	53	65	24	201	397	0.077	6.879	0.020	0.3571	0.0004	0.13971	0.00032	1968.5	3.6	2096.0	5.0	2223.6	7.8	13.3
10T	T,clr,pY,fg,fr	0.75A	20	45	21	7	240	99.3	0.040	5.911	0.076	0.3375	0.0011	0.12700	0.00139	1874.8	10.5	1962.8	22.4	2056.9	38.1	10.2

Z5611: Tonalite (98-tx-215)																						
1	Z,clr,co,sub,ro	M0	10	10	98	55	5	6103.2	0.082	13.043	0.016	0.5142	0.0005	0.18398	0.00008	2674.4	4.5	2682.8	2.4	2689.1	1.5	0.7
2	Z,clr,co,sub,pr,incl	M0	6	9	104	57	6	4608.1	0.086	12.754	0.015	0.5038	0.0005	0.18361	0.00008	2630.1	4.0	2661.7	2.2	2685.7	1.5	2.5
3	Z,clr,co,sub,pr	M0	6	5	129	71	13	1643.5	0.077	12.800	0.020	0.5060	0.0006	0.18346	0.00014	2639.7	5.4	2665.1	3.0	2684.4	2.6	2.0
4	Z,clr,co,sub,eq,incl	M0	4	4	155	86	3	5610.3	0.075	13.008	0.019	0.5143	0.0007	0.18342	0.00011	2675.2	5.6	2680.2	2.8	2684.1	2.0	0.4
5	Z, clr,clr,el,sub,pr,fr	M0	7	2	127	70	5	1939	0.109	12.477	0.020	0.4980	0.0007	0.18169	0.00012	2605.3	5.7	2641.0	3.0	2668.4	2.2	2.9
6T	clr,dBr,an	0.75A	8	155	141	78	647	1083.2	0.087	12.608	0.017	0.5066	0.0005	0.18049	0.00013	2642.2	4.1	2650.8	2.5	2657.4	2.4	0.7
7T	clr,Br,an	0.75A	17	103	81	47	750	350.5	0.220	11.453	0.032	0.4863	0.0005	0.17081	0.00038	2554.6	4.4	2560.8	5.2	2565.6	7.4	0.5
8T	T,clr,pBr,sub,tab	0.75A	19	24	132	82	589	162.2	0.421	10.625	0.063	0.4534	0.0008	0.16994	0.00085	2410.5	7.4	2490.9	11.0	2557.1	16.6	6.9
9T	T,clr,pBr,sub,tab	0.75A	18	44	27	14	110	327.1	0.130	10.662	0.028	0.4592	0.0007	0.16841	0.00033	2435.9	6.4	2494.1	4.9	2541.9	6.6	5.0
Z4839: Tonalite (96-txs-173a)																						
1	Z,clr,co,pr	NM1	2	4	35	19	4	1080.2	0.053	13.089	0.020	0.5135	0.0008	0.18487	0.00013	2671.5	6.9	2686.1	2.9	2697.1	2.4	1.2
2	Z,clr,co,pr	NM1	1	4	138	78	4	4601.4	0.079	13.148	0.013	0.5183	0.0005	0.18399	0.00006	2691.8	4.0	2690.3	1.9	2689.2	1.1	−0.1
3	Z,clr,co,ro,sub,pr	NM1	6	5	37	20	3	2077.9	0.059	12.898	0.017	0.5109	0.0006	0.18309	0.00007	2660.5	5.4	2672.2	2.5	2681.1	1.3	0.9
4	Z,clr,co,sub	NM1	4	4	201	110	6	3664.4	0.081	12.654	0.015	0.5034	0.0006	0.18232	0.00010	2628.3	4.8	2654.3	2.2	2674.1	1.9	2.1
5	Z,clr,co,sub,pr	NM1	6	6	218	120	5	8404.7	0.072	12.835	0.015	0.5106	0.0005	0.18230	0.00005	2659.3	4.6	2667.6	2.2	2673.9	1.0	0.7
6	Z,clr,co,pr	NM1	10	4	428	229	17	3060.1	0.050	12.611	0.013	0.5066	0.0005	0.18054	0.00006	2642.1	3.9	2651.0	1.9	2657.8	1.2	0.7
7T	T,dBr,an,fg,Abr	0.75A	21	69	192	85	153	2370.9	0.014	9.349	0.010	0.4389	0.0004	0.15449	0.00007	2345.6	3.3	2372.8	1.9	2396.3	1.5	2.5
8T	T,pBr,tur,sub,plates,Abr	0.75A	25	25	137	50	40	1932.5	0.020	7.546	0.008	0.3623	0.0003	0.15105	0.00008	1993.2	3.1	2178.5	2.0	2357.8	1.7	18.0
9T	T,dBr,an,fg,Abr	0.75A	18	44	52	17	53	905.1	0.019	5.486	0.009	0.3310	0.0003	0.12021	0.00012	1843.1	3.0	1898.4	2.7	1959.3	3.7	6.8
10T	T,pBr,tur,sub,plates,Abr	0.75A	15	19	31	10	29	436	0.016	5.413	0.014	0.3368	0.0005	0.11658	0.00023	1871.0	4.5	1886.9	4.5	1904.5	7.0	2.0
11T	T,dBr,an,fg,Abr	0.75A	15	39	37	12	55	555	0.044	5.154	0.012	0.3321	0.0003	0.11256	0.00019	1848.5	3.2	1845.1	3.8	1841.2	6.2	−0.5
Z5615: Tonalite (98-tx-275)																						
1	Z,clr,co,sub,ro,pr	Dia	5	4	94	54	5	2765.8	0.123	12.722	0.016	0.5080	0.0005	0.18163	0.00009	2648.1	4.4	2659.3	2.3	2667.8	1.6	0.9
2	Z,clr,co,sub,pr	Dia	2	2	90	51	4	1446	0.121	12.618	0.020	0.5077	0.0008	0.18024	0.00014	2646.9	6.6	2651.6	3.0	2655.1	2.6	0.4
3	Z,tur,co,el,pr	Dia	3	2	148	85	5	1670.2	0.137	12.609	0.019	0.5077	0.0007	0.18012	0.00012	2646.9	5.8	2650.9	2.8	2654.0	2.3	0.3
4	Z,clr,co,sub,ro,pr	Dia	2	3	174	99	4	3819	0.125	12.546	0.016	0.5062	0.0005	0.17977	0.00008	2640.3	4.4	2646.2	2.3	2650.7	1.6	0.5
5	Z,clr,co,sub,pr	dia	6	3	136	75	21	666.4	0.139	11.944	0.025	0.4876	0.0009	0.17766	0.00020	2560.2	8.1	2600.0	3.9	2631.1	3.7	3.3
6T	T,clr,lBr,an,fg,Abr	0.75A	16	120	59	61	159	1404.4	1.214	12.333	0.016	0.4996	0.0005	0.17903	0.00012	2612.1	3.9	2630.1	2.5	2643.9	2.2	1.5
7T	T,clr,Br,fg,Abr	0.75A	10	265	158	120	626	2073.9	0.599	12.208	0.015	0.4956	0.0005	0.17866	0.00010	2594.7	3.9	2620.5	2.4	2640.5	1.9	2.1
8T	T,clr,co,an,fg,Abr	0.75A	25	62	8	3	58	207.2	0.016	6.649	0.034	0.3684	0.0011	0.13089	0.00051	2021.9	9.9	2065.8	9.1	2110.0	13.6	4.9
Z4527: Augen Granite (96-txs-175)																						
1	Z,pr,sub, pBr	Dia	1	3	100	56	3	1729.1	0.098	12.657	0.023	0.5093	0.0009	0.18023	0.00012	2653.8	7.6	2654.5	3.5	2654.9	2.1	0.1
2	Z,pr,sub, tur	Dia	1	3	256	136	8	3479.6	0.061	12.144	0.015	0.4989	0.0006	0.17654	0.00007	2609.0	5.0	2615.6	2.3	2620.6	1.4	0.5
3	Z,fg,clr,pBr	Dia	4	5	48	27	6	1188.6	0.136	12.055	0.038	0.4991	0.0016	0.17519	0.00021	2609.7	13.4	2608.7	5.9	2607.8	3.9	−0.1
4	Z,pr,sub, pBr	Dia	9	1	1058	555	130	262.6	0.074	11.682	0.046	0.4890	0.0009	0.17326	0.00052	2566.3	7.6	2579.3	7.3	2589.4	10.0	1.1
5	Z,pr,sub, pBr	Dia	5	5	268	136	75	529.8	0.113	10.588	0.021	0.4594	0.0005	0.16716	0.00025	2436.8	4.1	2487.6	3.7	2529.4	4.9	4.4
6	Z,pr,sub, tur	Dia	9	6	185	86	19	1783.4	0.037	10.209	0.012	0.4468	0.0004	0.16572	0.00009	2381.1	3.7	2453.9	2.1	2514.9	1.9	6.4
7	Z,tur,fr,Br,tip	Dia	2	4	1139	519	83	1607.2	0.038	9.907	0.014	0.4416	0.0005	0.16271	0.00009	2357.8	4.5	2426.2	2.5	2484.0	1.9	6.1
Z5919: Diorite (99-txh-111)																						
1	Z,Co,Clr,Eq,Sub	Dia	1	26	92	59	4	19377	0.249	13.384	0.015	0.5227	0.0005	0.18570	0.00008	2710.7	4.0	2707.1	2.1	2704.5	1.4	−0.3
2	Z,Co,Clr,fFr,Pr,Tab	Dia	1	13	231	156	4	23956.6	0.325	13.279	0.015	0.5197	0.0005	0.18530	0.00008	2698.1	3.9	2699.7	2.1	2700.9	1.4	0.1
3	Z,Co,Clr,fFr,Tip,Abr,Dia	Dia	1	17	74	45	4	9992.1	0.201	13.048	0.015	0.5140	0.0005	0.18411	0.00008	2673.6	4.1	2683.1	2.2	2690.3	1.4	0.8
4T	T,Co,Clr,fFr,An,Abr	M-1A	28	167	7	2	316	91.9	0.037	4.670	0.076	0.3175	0.0013	0.10666	0.00146	1777.7	12.4	1761.8	27.1	1743.1	49.3	−2.3
5T	T,Co,Clr,fFr,An,Abr	M-1A	35	281	7	2	681	72.2	0.031	4.595	0.105	0.3156	0.0017	0.10557	0.00204	1768.4	16.8	1748.3	38.0	1724.3	69.5	−2.9
Z5687: South Channel granite (98-TXS-485)																						
1	Z,clr,co,eq,pr	M1	6	7	60	39	6	2309.2	0.278	13.113	0.016	0.5162	0.0005	0.18426	0.00011	2682.9	4.6	2687.8	2.3	2691.6	1.9	0.4
2	Z,clr,co,sub,pr	M1	10	7	40	27	6	1524.1	0.334	13.032	0.035	0.5136	0.0014	0.18402	0.00013	2672.1	11.6	2682.0	5.1	2689.4	2.3	0.8
3	Z,clr,co,sub,el,pr	M1	7	7	69	45	7	1603	0.308	12.806	0.019	0.5057	0.0007	0.18367	0.00012	2638.1	6.0	2665.5	2.9	2686.3	2.1	2.2
4	Z,clr,co,sub,eq,pr	M1	1	3	64	45	4	1571.4	0.418	12.972	0.019	0.5129	0.0007	0.18345	0.00010	2668.9	6.2	2677.6	2.8	2684.3	1.9	0.7

Table 1 (*Continued*)

Fraction	Description	Mag	# Grains	Wt. (μg)	U[2] (ppm)	Pb*[2] (ppm)	Pbc[1] (pg)	$\frac{^{206}Pb}{^{204}Pb}$[1]	$\frac{^{208}Pb}{^{206}Pb}$[2]	$\frac{^{207}Pb}{^{235}U}$[2]	$\pm\frac{^{207}Pb}{^{235}U}$	$\frac{^{206}Pb}{^{238}U}$[2]	$\pm\frac{^{206}Pb}{^{238}U}$	$\frac{^{207}Pb}{^{206}Pb}$[2]	$\pm\frac{^{207}Pb}{^{206}Pb}$	$\frac{^{206}Pb}{^{238}U}$	Apparent ages (Ma) $\pm\frac{^{206}Pb}{^{238}U}$	Apparent ages (Ma) $\frac{^{207}Pb}{^{235}U}$	$\pm\frac{^{207}Pb}{^{235}U}$	$\frac{^{207}Pb}{^{206}Pb}$	$\pm\frac{^{207}Pb}{^{206}Pb}$	Disc. (%)
5	Z,clr,co,sub,pr	M1	11	7	70	46	7	2236.4	0.323	12.679	0.017	0.5027	0.0005	0.18292	0.00010	2625.5	4.7	2656.1	2.5	2679.5	1.8	2.5
6T	T,clr,dBr,an,fg,Abr	0.75A	16	238	49	73	830	449.8	2.290	12.102	0.032	0.5013	0.0005	0.17509	0.00035	2619.4	4.5	2612.3	4.9	2606.9	6.7	−0.6
7T	T,clr,dBr,an,fg,Abr	0.75A	16	296	46	67	670	617.9	2.358	11.544	0.024	0.4825	0.0006	0.17352	0.00023	2538.1	5.1	2568.1	3.9	2591.9	4.4	2.5
8T	T,clr,Br,an,fg,Abr	0.75A	21	191	18	7	849	105.7	0.086	5.786	0.082	0.3521	0.0012	0.11919	0.00142	1944.6	11.2	1944.4	24.4	1944.2	42.1	0.0
9T	T,clr,co,an,fg,Abr	0.75A	22	116	7	2	159	125.8	0.020	5.214	0.051	0.3329	0.0010	0.11359	0.00093	1852.4	9.5	1854.9	16.6	1857.6	29.2	0.3
10T	T,clr,pBr,an,fg,Abr	0.75A	23	197	5	1	188	111.7	0.022	5.023	0.060	0.3272	0.0011	0.11133	0.00111	1825.0	10.9	1823.2	20.1	1821.3	35.8	−0.2
Z5641: Tonalite (98-txh-411a)																						
1	Z,clr,co,sub,ro,pr	Dia	1	6	50	32	3	1594.9	0.228	13.217	0.023	0.5197	0.0008	0.18447	0.00013	2697.7	7.1	2695.3	3.2	2693.5	2.3	−0.2
2	Z,clr,co,sub,el,pr	Dia	4	7	54	36	6	2094.3	0.326	13.026	0.018	0.5131	0.0006	0.18411	0.00011	2670.0	5.0	2681.5	2.6	2690.2	2.0	0.9
3	Z,clr,co,sub,pr	Dia	1	5	38	26	4	828.8	0.353	13.129	0.029	0.5175	0.0012	0.18400	0.00022	2688.5	9.9	2689.0	4.1	2689.3	3.9	0.0
4	Z,clr,co,eq,pr	Dia	4	11	56	36	9	2153.9	0.262	13.136	0.018	0.5182	0.0006	0.18386	0.00009	2691.5	5.0	2689.5	2.5	2688.0	1.6	−0.2
5	Z,clr,co,sub,tab,fr	Dia	1	7	27	16	3	1137.6	0.214	12.569	0.023	0.5033	0.0009	0.18114	0.00016	2627.8	7.7	2647.9	3.5	2663.3	2.9	1.6
6T	T,clr,dBr,an,fg,Abr	1A	15	305	203	109	736	1965.9	0.530	6.914	0.009	0.3722	0.0004	0.13471	0.00009	2039.8	3.4	2100.4	2.4	2160.3	2.3	6.5
7T	T,clr,dBr,an,fg,Abr	1A	15	287	187	96	678	1856	0.455	6.942	0.008	0.3740	0.0003	0.13461	0.00008	2048.2	3.2	2104.0	2.1	2159.0	2.0	6.0
8T	T, clr,py,an,fg,Abr	1A	43	38	70	24	75	768	0.041	5.542	0.010	0.3425	0.0003	0.11735	0.00015	1898.7	3.3	1907.1	3.2	1916.2	4.5	1.1
9T	T, clr,py,an,fg,Abr	1A	50	81	4	1	80	102.6	0.020	5.219	0.066	0.3320	0.0012	0.11401	0.00122	1848.0	11.6	1855.7	21.5	1864.3	38.0	1.0
Z5616: Granite (98-txh-411b)																						
1	Z,co,tur,fr,ro,pr	NM0	1	5	134	78	4	5674.5	0.153	12.890	0.015	0.5087	0.0005	0.18377	0.00008	2651.2	4.1	2671.7	2.2	2687.2	1.5	1.6
2	Z,clr,co,eq,eu	NM0	13	7	81	48	15	1190.7	0.243	11.980	0.017	0.4884	0.0005	0.17792	0.00013	2563.6	4.5	2602.9	2.7	2633.6	2.5	3.2
3	Z,clr,co,sub,tab	NM0	5	4	78	44	9	266.3	0.211	11.522	0.058	0.4754	0.0026	0.17579	0.00049	2507.1	22.6	2566.4	9.4	2613.5	9.2	4.9
4	Z,clr,co,el,pr	NM0	11	8	98	52	10	2335.7	0.163	10.958	0.013	0.4650	0.0004	0.17091	0.00010	2461.6	4.0	2519.6	2.3	2566.6	1.9	4.9
5	Z,clr,co,eu,pr	NM0	9	10	72	38	6	3253.4	0.160	10.852	0.013	0.4614	0.0004	0.17057	0.00008	2445.9	3.9	2510.6	2.2	2563.3	1.6	5.5
6T	T,clr,dBr,an,Abr	0.75A	11	41	146	56	462	284.4	0.219	5.274	0.024	0.3370	0.0005	0.11351	0.00042	1872.1	4.5	1864.7	7.6	1856.4	13.2	−1.0
7T	T,clr,co,an,fg,Abr	0.75A	40	92	8	3	143	114.2	0.101	4.843	0.056	0.3230	0.0011	0.10877	0.00106	1804.1	10.7	1792.4	19.5	1778.8	35.0	−1.6
8T	T,clr,pBr,an,fg,Abr	0.75A	30	116	70	25	1221	150.2	0.184	4.853	0.044	0.3240	0.0008	0.10865	0.00083	1809.1	7.8	1794.2	15.4	1776.8	27.6	−2.1
9T	T,clr,co,an,fg,Abr	0.75A	38	64	10	3	253	64.7	0.130	4.820	0.111	0.3240	0.0020	0.10790	0.00211	1809.2	19.2	1788.4	38.9	1764.2	69.9	−2.9
10T	clr,dBr,an,fg,Abr	0.75A	19	102	87	37	4512	57.8	0.343	5.116	0.155	0.3452	0.0024	0.10751	0.00278	1911.4	23.3	1838.8	51.6	1757.6	91.8	−10.1
Z5613: Granite (98-txh-389a)																						
1	Z,clr,co,tip	M1	3	2	900	295	29	975.7	0.029	5.290	0.009	0.3337	0.0003	0.11496	0.00012	1856.5	3.2	1867.3	2.9	1879.3	3.9	1.4
2	Z,clr,co,tip	M1	1	2	2808	939	305	454.2	0.053	5.212	0.016	0.3334	0.0004	0.11340	0.00027	1854.6	3.6	1854.6	5.2	1854.6	8.6	0.0
3	Z,clr,co,tip	M1	1	1	1355	437	44	910.5	0.024	5.139	0.009	0.3300	0.0003	0.11294	0.00013	1838.3	3.1	1842.5	3.0	1847.2	4.3	0.6
4	Z,clr,co,tip	M1	1	3	2088	688	97	1388.1	0.048	5.139	0.008	0.3301	0.0003	0.11291	0.00010	1838.8	3.0	1842.5	2.5	1846.8	3.2	0.5
5	Z,clr,tur,sub,pr	M0	8	3	1266	402	237	341.2	0.053	4.928	0.020	0.3166	0.0004	0.11291	0.00037	1772.9	3.9	1807.1	6.8	1846.8	11.8	4.6
6	Z,tur,co,el,pr	M1	7	10	1750	568	535	684.5	0.037	5.069	0.011	0.3286	0.0003	0.11187	0.00018	1831.7	3.2	1830.9	3.8	1830.0	5.9	−0.1
7	Z,clr,co,eu,tab	M0	3	5	1486	467	112	1326.6	0.036	4.859	0.007	0.3189	0.0003	0.11050	0.00010	1784.3	2.8	1795.1	2.5	1807.7	3.3	1.5
8	Z,tur,co,el,pr	M1	8	9	1551	485	578	502.5	0.035	4.826	0.014	0.3174	0.0003	0.11027	0.00026	1776.9	3.4	1789.4	5.0	1803.9	8.5	1.7
9	Z,clr,co,tip	M1	1	4	2900	882	936	251	0.050	4.573	0.025	0.3053	0.0005	0.10863	0.00049	1717.6	4.9	1744.4	9.2	1776.6	16.5	3.8
10T	T,clr,Br,an,fg,Abr	0.75A	13	74	112	39	1419	137.5	0.091	4.993	0.058	0.3379	0.0009	0.10716	0.00106	1876.7	8.8	1818.2	19.6	1751.7	35.7	−8.2
11T	T,clr,dBr,an,fg,Abr	0.75A	12	79	118	42	1436	157.2	0.065	5.151	0.050	0.3492	0.0008	0.10698	0.00088	1930.7	7.9	1844.5	16.5	1748.6	29.9	−12.1
12T	T,clr,dBr,an,fg,Abr	NM1	11	112	186	68	3332	147.9	0.135	5.037	0.048	0.3418	0.0008	0.10686	0.00085	1895.5	8.1	1825.5	16.1	1746.6	29.0	−9.9
13T	T,clr,pBr,an,fg;Abr	0.75A	15	45	39	12	332	117.4	0.085	4.464	0.052	0.3074	0.0009	0.10530	0.00102	1728.1	9.3	1724.3	19.2	1719.6	35.3	−0.6
14T	T,clr,co,an,fg,Abr	0.75A	23	35	173	44	408	256.1	0.038	3.562	0.020	0.2603	0.0004	0.09923	0.00046	1491.4	4.5	1541.0	8.9	1609.7	17.1	8.2
Z5614: Granite (98-txh-389b)																						
1	Z,clr,co,tab,fg	Dia	1	3	533	182	12	2912.9	0.126	4.914	0.007	0.3210	0.0003	0.11102	0.00007	1794.7	3.2	1804.7	2.2	1816.2	2.4	1.4
2	Z,clr,co,an,fg	Dia	1	11	296	105	10	6518.2	0.169	4.950	0.006	0.3235	0.0003	0.11097	0.00005	1806.8	2.8	1810.7	1.9	1815.3	1.6	0.5
3	Z,clr,co,an,fg	Dia	1	9	468	173	9	9676.7	0.225	4.901	0.006	0.3206	0.0003	0.11086	0.00005	1792.8	2.8	1802.5	1.9	1813.6	1.6	1.3
4	Z,clr,co,tab,fg	Dia	1	5	290	107	5	3830	0.217	4.928	0.006	0.3238	0.0004	0.11039	0.00008	1808.2	3.6	1807.1	2.2	1805.8	2.6	−0.2

5T	T,clr,an,Br,Abr	0.5A	13	151	172	97	423	1237.2	0.934	4.878	0.008	0.3201	0.0003	0.11052	0.00011	1790.2	2.9	1798.5	2.7	1808.1	3.6	1.1
6T	T,clr,an,Br,Abr	0.5A	9	256	187	106	719	1355.4	0.930	4.909	0.007	0.3222	0.0003	0.11048	0.00010	1800.7	2.9	1803.8	2.6	1807.3	3.3	0.4
7T	T,clr,an,Br.Abr	0.5A	9	137	148	79	377	1085.5	0.820	4.868	0.009	0.3196	0.0003	0.11047	0.00014	1787.8	3.0	1796.7	3.0	1807.1	4.5	1.2
8T	T,clr,an,Br,Abr	0.5A	10	247	197	106	715	1369.4	0.828	4.872	0.008	0.3202	0.0003	0.11034	0.00010	1790.7	3.2	1797.4	2.7	1805.1	3.4	0.9
Z5915: Monzogranite (98-txh-414)																						
1	Z,Co,Clr,Eu,Pr	Dia	2	10	83	33	7	2417.8	0.281	5.062	0.007	0.3280	0.0004	0.11194	0.00008	1828.6	3.7	1829.8	2.4	1831.2	2.7	0.2
2	Z,Co,Clr,Eu,St	Dia	3	6	85	35	5	2187.5	0.325	5.052	0.008	0.3275	0.0004	0.11188	0.00009	1826.1	4.0	1828.0	2.6	1830.2	3.0	0.3
3	Z,Co,Clr,El,Eu,Pr	Dia	3	8	68	27	5	2454	0.289	5.038	0.008	0.3270	0.0005	0.11175	0.00012	1823.7	4.9	1825.7	2.8	1828.1	4.0	0.3
4	Z,Co,Clr,Eq,Sub	Dia	4	21	67	27	84	363.1	0.290	5.101	0.019	0.3298	0.0004	0.11218	0.00033	1835.0	10.5	1837.4	4.0	1836.3	6.2	−0.2
5T	T,dBr,Clr,An,Abr	0.75A	14	220	219	109	2899	339.6	0.723	4.836	0.021	0.3143	0.0004	0.11159	0.00040	1761.9	4.1	1791.1	7.4	1825.4	13.0	4.0
6T	T,Br,Clr,An,Abr	0.75A	15	135	199	99	1121	500.5	0.668	5.003	0.015	0.3254	0.0004	0.11149	0.00026	1816.2	3.6	1819.8	5.0	1823.8	8.3	0.5
7T	T,dBr,Clr,An,Abr	0.75A	1	16	230	131	683	125.4	0.900	5.021	0.059	0.3272	0.0009	0.11128	0.00111	1824.9	9.0	1822.8	19.9	1820.5	35.6	−0.3
8T	T,pBr,Clr,An,Abr	0.75A	23	87	37	14	292	233.2	0.274	4.770	0.027	0.3179	0.0005	0.10881	0.00051	1779.6	5.2	1779.6	9.6	1779.6	17.1	0.0
Z4685: Granite (96-Tx-027)																						
1	Z,clr,pBr,fg	NM1	1	6	40	13	9	540.4	0.012	5.115	0.012	0.3250	0.0005	0.11414	0.00018	1814.1	5.3	1838.5	3.8	1866.3	5.7	3.2
2	Z,clr,pBr,fg	NM1	2	9	21	7	9	480.7	0.010	5.165	0.013	0.3293	0.0006	0.11377	0.00022	1834.9	5.6	1846.9	4.4	1860.4	7.0	1.6
3	Z,clr/tur,co,sub,pr,fr	NM1	7	5	143	59	10	1393.9	0.362	5.033	0.006	0.3268	0.0003	0.11170	0.00007	1822.8	3.2	1824.9	2.2	1827.3	2.4	0.3
4T	T,clr,co,fg,fr;Abr	0.75A	20	161	34	12	878	136.6	0.157	4.819	0.047	0.3082	0.0008	0.11341	0.00094	1731.8	7.6	1788.3	16.5	1854.8	29.5	7.6
5T	T,clr,dBr,fg,fr	0.75A	19	53	50	17	205	263.2	0.137	4.653	0.023	0.3084	0.0005	0.10940	0.00044	1733.1	4.5	1758.8	8.2	1789.5	14.7	3.6
6T	T,clr,pBr,fg;Abr	0.75A	16	43	71	24	225	275.4	0.192	4.596	0.022	0.3071	0.0004	0.10854	0.00042	1726.4	4.3	1748.6	7.8	1775.1	14.1	3.1

Description: Z, zircon; T, titanite; ovg, overgrowth; fg, fragment; eu, euhedral; an, anhedral; ro, round; sub, subhedral; eq, equant; pr, prismatic; st, stubby prism; el, elongate; Tab, tabular; res, resorbed; clr, clear; tur, turbid; co, colourless; bl, black; Br, brown; pBr, pale brown; y, yellow; pY, pale yellow; dk, dark; op, opaque; irr, irregular shape; Abr, abraded. Mag refers to magnetic fraction on Frantz magnetic separator. Dia, diamagnetic; 0.5A, magnetic at given current 10° slope; NM1, non-magnetic at given sideslope; M1, magnetic at given side slope (°). Concentration uncertainty varies with sample weight: >10% for sample weights <10 μg, <10% for sample weights above 10 μg. Asterisk (*), radiogenic Pb; Pc, total common Pb in analysis corrected for spike and fractionation. Atomic ratios corrected for spike, fractionation, blank and initial common Pb, except $^{206}Pb/^{204}Pb$ ratio corrected for spike and fractionation only. Errors are one sigma absolute. Blank composition (atomic proportions): 208Pb = 0.5197; 207Pb = 0.2136; 206Pb = .2529; 204Pb = .0139. Common Pb correction based on Cumming and Richards (1975) model. Errors on apparent ages given at two-sigma level in Ma.

Table 2
SHRIMP analytical data

Analyses number	U (ppm)	Th (ppm)	Th (U)	Pb* (ppm)	^{204}Pb (ppb)	$\frac{^{204}Pb}{^{206}Pb}$	$\pm\frac{^{204}Pb}{^{206}Pb}$	$f(206)^{204}$	$\frac{^{208*}Pb}{^{206*}Pb}$	$\pm\frac{^{208}Pb}{^{206}Pb}$	$\frac{^{207*}Pb}{^{235}U}$	$\pm\frac{^{207}Pb}{^{235}U}$	$\frac{^{206*}Pb}{^{238}U}$	$\pm\frac{^{206}Pb}{^{238}U}$	Corr Coeff	$\frac{^{207*}Pb}{^{206*}Pb}$	$\pm\frac{^{207}Pb}{^{206}Pb}$	Apparent ages (Ma)				Disc. (%)
																		$\frac{^{206}Pb}{^{238}U}$	$\pm\frac{^{206}Pb}{^{238}U}$	$\frac{^{207}Pb}{^{206}Pb}$	$\pm\frac{^{207}Pb}{^{206}Pb}$	
4409																						
4409-5.2	1529	456	0.31	956	5	0.00001	0.00001	0.0001	0.086	0.001	14.935	0.260	0.5695	0.0090	0.9466	0.19021	0.00108	2906	37	2744	9	−5.9
4409-4.2	108	59	0.56	65	6	0.00013	0.00005	0.0022	0.151	0.004	13.506	0.268	0.5204	0.0090	0.9176	0.18823	0.00149	2701	38	2727	13	0.9
4409-11.1	534	212	0.41	317	6	0.00002	0.00001	0.0004	0.113	0.003	13.901	0.701	0.5299	0.0144	0.6373	0.19025	0.00745	2741	61	2744	66	0.1
4409-10.2	85	44	0.53	49	0	0.00001	0.00001	0.0002	0.150	0.007	12.585	0.258	0.4952	0.0092	0.9471	0.18433	0.00122	2593	40	2692	11	3.7
4409-12.1	527	121	0.24	289	7	0.00003	0.00002	0.0005	0.065	0.001	13.307	0.287	0.5078	0.0105	0.9826	0.19004	0.00077	2647	45	2743	7	3.5
4409-1.1	864	589	0.70	538	12	0.00003	0.00001	0.0005	0.194	0.001	13.736	0.214	0.5216	0.0075	0.9617	0.19099	0.00082	2706	32	2751	7	1.6
4409-2.1	1932	642	0.34	1173	4	0.00000	0.00000	0.0001	0.096	0.001	14.267	0.324	0.5496	0.0104	0.8938	0.18828	0.00193	2823	44	2727	17	−3.5
4409-4.1	527	183	0.36	308	7	0.00003	0.00002	0.0005	0.100	0.002	13.760	0.216	0.5269	0.0077	0.9640	0.18941	0.00080	2728	33	2737	7	0.3
4409-5.1	1648	520	0.33	993	8	0.00001	0.00001	0.0002	0.091	0.001	14.394	0.221	0.5463	0.0082	0.9933	0.19111	0.00034	2810	34	2752	3	−2.1
4409-8.1	1152	365	0.33	661	5	0.00001	0.00001	0.0002	0.088	0.001	13.383	0.227	0.5238	0.0079	0.9332	0.18530	0.00114	2715	33	2701	10	−0.5
4409-9.1	554	179	0.33	314	24	0.00010	0.00002	0.0017	0.091	0.001	13.502	0.226	0.5142	0.0078	0.9492	0.19046	0.00101	2674	33	2746	9	2.6
4409-11.1	719	162	0.23	399	3	0.00001	0.00001	0.0002	0.062	0.001	13.537	0.395	0.5144	0.0102	0.7612	0.19086	0.00364	2675	44	2750	32	2.7
4327																						
4327-32.1	162	1	0.01	53	2	0.00004	0.00007	0.0007	0.003	0.003	5.440	0.127	0.3411	0.0055	0.7777	0.11566	0.00170	1892	27	1890	27	−0.1
4327-8.1	491	8	0.02	158	8	0.00005	0.00002	0.0010	0.003	0.001	5.348	0.095	0.3343	0.0053	0.9417	0.11600	0.00070	1859	26	1896	11	1.9
4327-64.1	548	7	0.01	178	1	0.00000	0.00002	0.0001	0.004	0.002	5.396	0.096	0.3364	0.0054	0.9365	0.11632	0.00073	1869	26	1900	11	1.6
4327-28.1	141	1	0.01	46	0	0.00001	0.00001	0.0002	0.003	0.001	5.541	0.104	0.3392	0.0057	0.9344	0.11849	0.00080	1883	27	1934	12	2.6
4327-45.1	271	2	0.01	86	1	0.00001	0.00001	0.0002	0.002	0.000	5.412	0.109	0.3301	0.0053	0.8664	0.11893	0.00120	1839	26	1940	18	5.2
4327-44.1	19	0	0.01	6	2	0.00043	0.00030	0.0075	0.006	0.012	5.142	0.278	0.3129	0.0081	0.5797	0.11917	0.00530	1755	40	1944	82	9.7
4327-61.1	213	1	0.00	68	2	0.00003	0.00007	0.0006	0.002	0.003	5.456	0.121	0.3314	0.0057	0.8365	0.11940	0.00147	1845	27	1947	22	5.2
4327-38.1	35	0	0.00	11	1	0.00012	0.00047	0.0022	0.008	0.017	5.900	0.405	0.3402	0.0080	0.4552	0.12577	0.00775	1888	39	2040	113	7.5
4327-2.2	23	2	0.09	7	5	0.00077	0.00020	0.0134	–	0.008	5.876	0.218	0.3290	0.0052	0.5342	0.12953	0.00409	1834	25	2092	57	12.3
4327-1.1	19	0	0.01	7	2	0.00027	0.00039	0.0046	0.003	0.015	7.220	0.596	0.3657	0.0064	0.3312	0.14319	0.01124	2009	30	2266	142	11.3
4327-8.3	264	3	0.01	101	3	0.00003	0.00001	0.0005	0.002	0.001	7.842	0.122	0.3859	0.0053	0.9226	0.14740	0.00089	2104	24	2316	10	9.2
4327-38.2	176	1	0.00	71	4	0.00007	0.00003	0.0012	0.000	0.001	8.469	0.174	0.4065	0.0077	0.9587	0.15111	0.00089	2199	35	2358	10	6.8
4327-59.1	301	2	0.01	137	3	0.00002	0.00001	0.0004	0.001	0.001	10.146	0.142	0.4561	0.0057	0.9419	0.16135	0.00077	2422	25	2470	8	1.9
4327-57.1	233	3	0.01	108	4	0.00005	0.00002	0.0008	0.001	0.001	10.356	0.222	0.4621	0.0058	0.6811	0.16255	0.00258	2449	26	2482	27	1.4
4327-8.2	220	1	0.01	96	0	0.00000	0.00005	0.0001	0.002	0.002	9.878	0.197	0.4374	0.0071	0.8777	0.16378	0.00158	2339	32	2495	16	6.3
4327-18.1	911	5	0.01	438	3	0.00001	0.00001	0.0001	0.002	0.000	11.089	0.179	0.4781	0.0074	0.9798	0.16823	0.00055	2519	32	2540	5	0.8
4327-28.3	68	25	0.37	36	3	0.00009	0.00007	0.0016	0.107	0.003	11.755	0.202	0.4760	0.0069	0.8969	0.17911	0.00137	2510	30	2645	13	5.1
4327-4.1	164	83	0.52	95	2	0.00003	0.00002	0.0006	0.144	0.002	12.795	0.197	0.5104	0.0071	0.9442	0.18180	0.00093	2658	30	2669	8	0.4
4327-18.3	93	35	0.39	51	4	0.00011	0.00003	0.0019	0.107	0.002	12.372	0.183	0.4933	0.0067	0.9560	0.18190	0.00080	2585	29	2670	7	3.2
4327-52.1.2	63	21	0.34	35	0	0.00001	0.00001	0.0002	0.095	0.003	12.842	0.196	0.5085	0.0072	0.9613	0.18315	0.00078	2650	31	2682	7	1.2
4327-28.2	81	31	0.40	44	6	0.00016	0.00011	0.0028	0.115	0.005	12.460	0.282	0.4898	0.0086	0.8467	0.18450	0.00224	2570	37	2694	20	4.6
4327-52.1	66	23	0.35	37	1	0.00002	0.00006	0.0003	0.097	0.003	12.872	0.271	0.5045	0.0072	0.7564	0.18505	0.00257	2633	31	2699	23	2.4
4327-9.1	122	51	0.43	69	1	0.00003	0.00002	0.0005	0.121	0.001	12.888	0.268	0.5045	0.0072	0.7627	0.18528	0.00251	2633	31	2701	23	2.5
4327-18.2	86	31	0.37	47	4	0.00011	0.00008	0.0019	0.101	0.004	12.653	0.305	0.4945	0.0084	0.7817	0.18558	0.00281	2590	36	2703	25	4.2
5642																						
5642-1.1	113	32	0.29	62	0	0.00001	0.00004	0.00009	0.085	0.002	12.786	0.219	0.5037	0.0069	0.8623	0.18410	0.00161	2630	30	2690	15	2.2
5642-5.1	502	88	0.18	273	1	0.00000	0.00001	0.00005	0.050	0.001	12.848	0.168	0.5124	0.0065	0.9837	0.18187	0.00043	2667	28	2670	4	0.1
5642-8.1	128	92	0.74	78	2	0.00004	0.00002	0.00062	0.212	0.004	12.846	0.196	0.5112	0.0071	0.9506	0.18224	0.00087	2662	30	2673	8	0.4
5642-11.1	119	89	0.78	73	1	0.00003	0.00002	0.00045	0.214	0.002	12.915	0.196	0.5146	0.0070	0.9403	0.18202	0.00095	2676	30	2671	9	−0.2
5642-12.1	107	67	0.65	63	0	0.00000	0.00002	0.00007	0.176	0.002	12.806	0.180	0.5076	0.0065	0.9482	0.18298	0.00082	2646	28	2680	7	1.3
5642-21.1	72	36	0.53	42	2	0.00006	0.00004	0.00109	0.144	0.004	12.852	0.230	0.5137	0.0076	0.8812	0.18145	0.00155	2672	32	2666	14	−0.2
5642-25.1	32	14	0.44	18	1	0.00008	0.00006	0.00139	0.131	0.004	12.813	0.273	0.5106	0.0096	0.9281	0.18200	0.00145	2659	41	2671	13	0.4

5687																						
5687-1.1	101	131	1.34	70	0	0.00001	0.00001	0.00017	0.368	0.002	13.307	0.188	0.5221	0.0067	0.9511	0.18485	0.00081	2708	29	2697	7	−0.4
5687-5.1	40	41	1.05	26	1	0.00003	0.00012	0.00054	0.295	0.005	13.000	0.254	0.5093	0.0071	0.7900	0.18513	0.00223	2654	30	2699	20	1.7
5687-19.1	64	82	1.32	44	0	0.00001	0.00001	0.00017	0.366	0.004	13.121	0.204	0.5196	0.0075	0.9586	0.18316	0.00082	2697	32	2682	7	−0.6
5687-31.1	401	258	0.66	246	2	0.00001	0.00001	0.00021	0.186	0.001	13.163	0.176	0.5204	0.0066	0.9760	0.18344	0.00054	2701	28	2684	5	−0.6
5687-46.1	69	76	1.15	46	0	0.00001	0.00001	0.00017	0.330	0.004	12.867	0.263	0.5090	0.0083	0.8615	0.18334	0.00192	2652	36	2683	17	1.2
5687-58.1	92	31	0.35	53	0	0.00001	0.00001	0.00017	0.098	0.001	13.356	0.197	0.5233	0.0072	0.9671	0.18512	0.00070	2713	31	2699	6	−0.5
5687-63.1	220	311	1.46	152	1	0.00001	0.00001	0.00017	0.408	0.006	12.557	0.333	0.5038	0.0099	0.8138	0.18076	0.00281	2630	43	2660	26	1.1
5687-72.1	116	96	0.85	72	1	0.00001	0.00001	0.00017	0.235	0.002	12.892	0.183	0.5052	0.0067	0.9694	0.18508	0.00065	2636	29	2699	6	2.3
5687-85.1	41	35	0.89	25	4	0.00023	0.00007	0.00393	0.237	0.005	12.824	0.223	0.5118	0.0072	0.8745	0.18174	0.00154	2664	31	2669	14	0.2
5687-78.1	121	132	1.12	79	1	0.00001	0.00001	0.00017	0.311	0.002	12.977	0.189	0.5097	0.0069	0.9586	0.18464	0.00077	2656	29	2695	7	1.5
5687-89.1	130	201	1.60	93	2	0.00004	0.00002	0.00074	0.444	0.005	12.968	0.183	0.5106	0.0066	0.9553	0.18420	0.00077	2659	28	2691	7	1.2
5687-87.1	75	78	1.08	49	1	0.00003	0.00006	0.00059	0.301	0.004	13.029	0.224	0.5116	0.0069	0.8545	0.18471	0.00166	2663	30	2696	15	1.2
5687-93.1	226	445	2.04	174	1	0.00001	0.00001	0.00017	0.570	0.003	12.921	0.177	0.5105	0.0065	0.9600	0.18356	0.00071	2659	28	2685	6	1.0

Notes (see Stern, 1997): analyses number: sample name-grain number.spot number.analyses number. Uncertainties reported at 1s (absolute) and are calculated by numerical propagation of all known sources of error. $f206^{204}$ refers to mole fraction of total 206Pb that is due to common Pb, calculated using the 204Pb-method; common Pb composition used is the surface blank (4/6: 0.05770; 7/6: 0.89500; 8/6: 2.13840). Asterisk (*) refers to radiogenic Pb (corrected for common Pb). Discordance relative to origin = 100 × (1 − (206Pb/238U age)/(207Pb/206Pb age)). Calibration standard 6266; U = 910 ppm; age = 559 Ma; 206Pb/238U = 0.09059. Error in 206Pb/238U calibration 1.2% (see Stern and Amelin, 2003). Th/U calibration: $F = 0.03900 \times \mathrm{UO} + 0.85600$.

Table 3
Summary of U–Pb age interpretations

Map ref. #	Map unit	Unit	GSC lab #	Sample #	UTM (zone 15; NAD27)		Mineral	Inter.	Age (Ma)	+	–	Lower intercept	MSWD	Method	Comment
					Easting	Northing									
MacQuoid belt: supracrustal rocks															
4	Afv	Massive felsic volcanic	Z4409	96TXV078	425225	7055576	Zircon	IC max	2745	8.0	8.0		2.9	WA	Ion probe ($n = 10$)
									2744	12.0	8.0	500	13.9	LR	Fraction 5 excluded
8	Afv	Felsic volcanic	Z5491	98TXJ184	439784	7063256	Zircon	IC	2682	3.3	1.6	−53	0.37	LR	1–4
	Afv	Felsic volcanic	Z5642	98TXJ109	427245	7055843	Zircon	IC max	2672	5.5	5.5	–	–	WA	Ion probe
20	Afv	Dacite breccia	Z4327	93HVAK643B	456329	7090165	Zircon	IC	2674	12.0	12.0			WA	Ion probe
							Zircon		2650	20.0	17.0	1952	1.33	LR	1,4, 6 excl
							Titanite	MC	1900	2.1	2.1	–	–	WA	8T, 9T
2	Av	Polymictic conglomerate	Z4497	96TX088	408240	7062498	Zircon	Detrital				–	–		2890–3400 detrital grains
MacQuoid homocline: intrusive rocks															
6	Atp	Tonalite	Z4532	96TX022	431945	7037705	Zircon	IC	2678	2.2	2.0	802	0.46	LR	#5 excl.
5	Atp	Tonalite	Z5611	98TX215	430186	7051339	Zircon	IC	2684	2.6	2.0	−209	0.47	LR	#1 and 5 excl.
	Atp	Tonalite (mylonite)	Z4839	96TXS173a	413403	7025440	Zircon	IC max	2689	1.1	1.1	–	–	SC	Youngest concordant age
							Titanite	–	1840	6.2	6.2	–	–	SC	Concrdat titanite
7	Atp	Tonalite	Z5615	98TX275	446206	7049954	Zircon	IC	2655	2.8	2.3	1091	1.36	LR	#1 excl.
1	Ag	Augen granite	Z4527	96TXV175	403281	7067379	Zircon	IC	2609	10.4	9.0	1571	0.40	LR	3, 4, 5, 7
3	Pgr	granite	Z4685	96TX027	420756	7064702	Zircon	IC max	1827	2.4	2.4	–	–	SC	Single concordant grain, inherited component
Cross Bay complex: intrusive rocks															
14	Adi	Hb-bt diorite	Z5919	99TXH111	485071	7071692	Zircon	IC	2701	2.1	2.0	1528	1.56	LR	1–3
12	Ag	Granite	Z5687	98TXS485	453305	7080734	Zircon	IC	2692	4.2	4.2		1.10	WA	Ion probe
									2694	6.5	5.0	906	4.14	LR	#3 excl.
13	Ag	4.00	Z5641	98TXH411a	460302	7079992	Zircon	IC	2690	4.0	4.0	–	5.20	WA	1–4
13	Ag	Granite pegmatite vein	Z5616	98TXH411b	460302	7079992	Zircon	Inh	2725			–	–	LR	Inherited grains
15	Pgr	Granite	Z5613	98TXH389a	483800	7090000	Zircon	IC	1828	10.3	7.0	1049	0.05	LR	6–9
15	Pgr	Granite	Z5614	98TXH389b	483800	7090000	Zircon and titanite	IC	1807	3.0	2.0	–143	0.60	LR	Pinned by concordant zircon
							Titanite	–	1807	14.0	4.0	93	0.80	LR	5T–8T
16	Pgr	Monzogranite	Z5915	98TXH414	493561	7085668	Zircon	IC	1830	1.7	1.7	–	0.94	WA	1–4
							Titanite	–	1824	7.0	7.0	–	–	LR	5T–7T

Map unit reference numbers correspond to samples indicated in Tella et al. (2001). *Interpretations*: IC, igneous crystallization; IC max, estimate of maximum crystallization age (generally based on age of youngest concordant zircon); Inh, age estimate of inherited zircon in sample; IC est, estimated igneous crystallization age; MC, metamorphic crystallization. *Methods*: LR, linear regression (modified York, 1969); WA, weighted average $^{207}Pb/^{206}Pb$ age (Ludwig, 2001); SC, single concordant date. MSWD, mean square of the weighted deviates for LR and WA methods; lower intercept, age in Ma of lower intercept of regression.

abraded (Krogh, 1982) prior to analyses by isotope dilution thermal ionization mass spectrometry (ID-TIMS). Monazite fractions were not abraded. Analytical methods for thermal ionization U–Pb analyses of zircon and monazite are summarized in Roddick et al. (1987) and Parrish et al. (1987) and for titanite in Davis et al. (1997). Analytical errors are determined based on error propagation methods of Roddick (1987).

SHRIMP analytical procedures followed those described by Stern (1997), with standards and U–Pb calibration methods following Stern and Amelin (2003). Zircons were cast in 2.5 cm diameter epoxy mounts along with fragments of the GSC laboratory standard zircon (Z6266, with $^{206}Pb/^{238}U$ age = 559 Ma). The midsections of the zircons were exposed using 9, 6 and 1 μm diamond compound, and the internal features of the zircons (such as zoning, structures, alteration, etc.) were characterized with backscattered electrons (BSE) utilizing a Cambridge Instruments scanning electron microscope. Mount surfaces were evaporatively coated with 10 nm of high purity Au. Analyses were conducted using an $^{16}O^-$ primary beam, projected onto the zircons at 10 kV. The sputtered area used for analysis was ca. 20 μm in diameter with a beam current of ca. 6.5 nA. The count rates of ten isotopes of Zr^+, U^+, Th^+ and Pb^+ in zircon were sequentially measured with a single electron multiplier and a pulse counting system with deadtime of 28 ns. Mass resolution was 5120 (1%). Off-line data processing was accomplished using customized in-house software. The 1σ external errors of $^{206}Pb/^{238}U$ ratios reported in Table 2 incorporate a ±1.0% error in calibrating the standard zircon (see Stern and Amelin, 2003). No fractionation correction was applied to the Pb-isotope data; common Pb correction utilized the measured $^{204}Pb/^{206}Pb$.

Precise sample locations and interpreted age summaries are given in Table 3. A modified (York, 1969) regression method was used to calculate upper and lower concordia intercept ages (Table 3). Weighted mean ages were calculated using Isoplot v. 3.0 (Ludwig, 2001).

5.2. *Depositional ages of volcanic belts*

Three samples of felsic volcanic rocks from the principal volcanic belt (Z4409, Z5491 and Z5642; Fig. 3), and one dacitic breccia from the northern extension on the South Channel of Chesterfield Inlet (Z4327), were collected to evaluate the depositional age of volcanic rocks. In addition, a sample of a distinctive polymictic conglomerate (Z4497) intercalated with mafic volcanic rocks from the PVB was collected to evaluate the detrital component.

Sample Z4409 is from a massive, 5–7 m thick, white to buff weathering quartz ± plagioclase porphyritic felsic volcanic unit from within the principal volcanic belt (Fig. 2). The unit occurs within amphibolite-facies, massive to locally pillowed mafic volcanic rocks. Flow banding observed within the marginal zone of the felsic layer is interpreted to indicate an extrusive origin, and thus the age of the layer dates the age of volcanism in this area. Only a small number of zircons were recovered, comprising a dominant population of small (<100 μm) euhedral, brown grains exhibiting prominent oscillatory growth zoning under optical microscope. Five analyses yield a range of discordant ID-TIMS dates between 2721 and 2742 Ma (Table 1; Fig. 5A). The analyses do not define a unique discordia array. One analyses is concordant at 2739 ± 8 Ma and three others are discordant with similar (#1–4) $^{207}Pb/^{206}Pb$ ages of between 2733 and 2742 Ma. Linear regression of these four analyses gives an upper intercept of 2744 + 12/−8 Ma and a lower intercept of ∼0.5 Ga (MSWD = 13.9; Tables 1 and 2). Ion microprobe analyses of 10 zircon grains yield ages between 2700 and 2751 Ma with a weighted mean age of 2745 ± 8 (MSWD = 2.9), similar to the age of the concordant TIMS results (Tables 2 and 3). One grain has a younger $^{207}Pb/^{206}Pb$ age of 2700 ± 22 Ma. However, as only a small number of zircon was recovered from this sample it is possible that the grains are dominantly inherited, and thus the 2745 ± 8 Ma date provides a maximum age estimate for the rock.

Sample Z5491 is a sample of quartz-plagioclase porphyritic felsic breccia, located in the principal volcanic belt approximately 15 km to the NE of sample Z4409 (Fig. 2). Zircon occurs as clear colourless, prismatic to equant crystals with slightly resorbed faces. Four multigrain analyses yield concordant to discordant results that provide an upper intercept of 2682 + 3/−2 Ma (Fig. 5B; Table 3), interpreted as the crystallization age of the volcanic rock.

Sample Z5642 is from a quartz-plagioclase-phyric rhyodacite within a unit of felsic volcanic rocks with minor mafic volcanic rocks within the principal volcanic belt. Many of the rocks in the sequence are fragmental. The sampled unit is very fine-grained and massive. Six analyses of euhedral prismatic grains yield variably discordant ID-TIMS data with a range of apparent ages from ∼2.66 to 2.68 Ga (Fig. 5E). Ion microprobe analyses of seven grains yield a weighted mean age of 2671.6 ± 5.5 Ma (Table 3), interpreted as the crystallization age of the volcanic rock. This age is slightly older than the youngest $^{207}Pb/^{206}Pb$ ID-TIMS result at 2661 ± 3 Ma and provides a maximum age estimate for the rock.

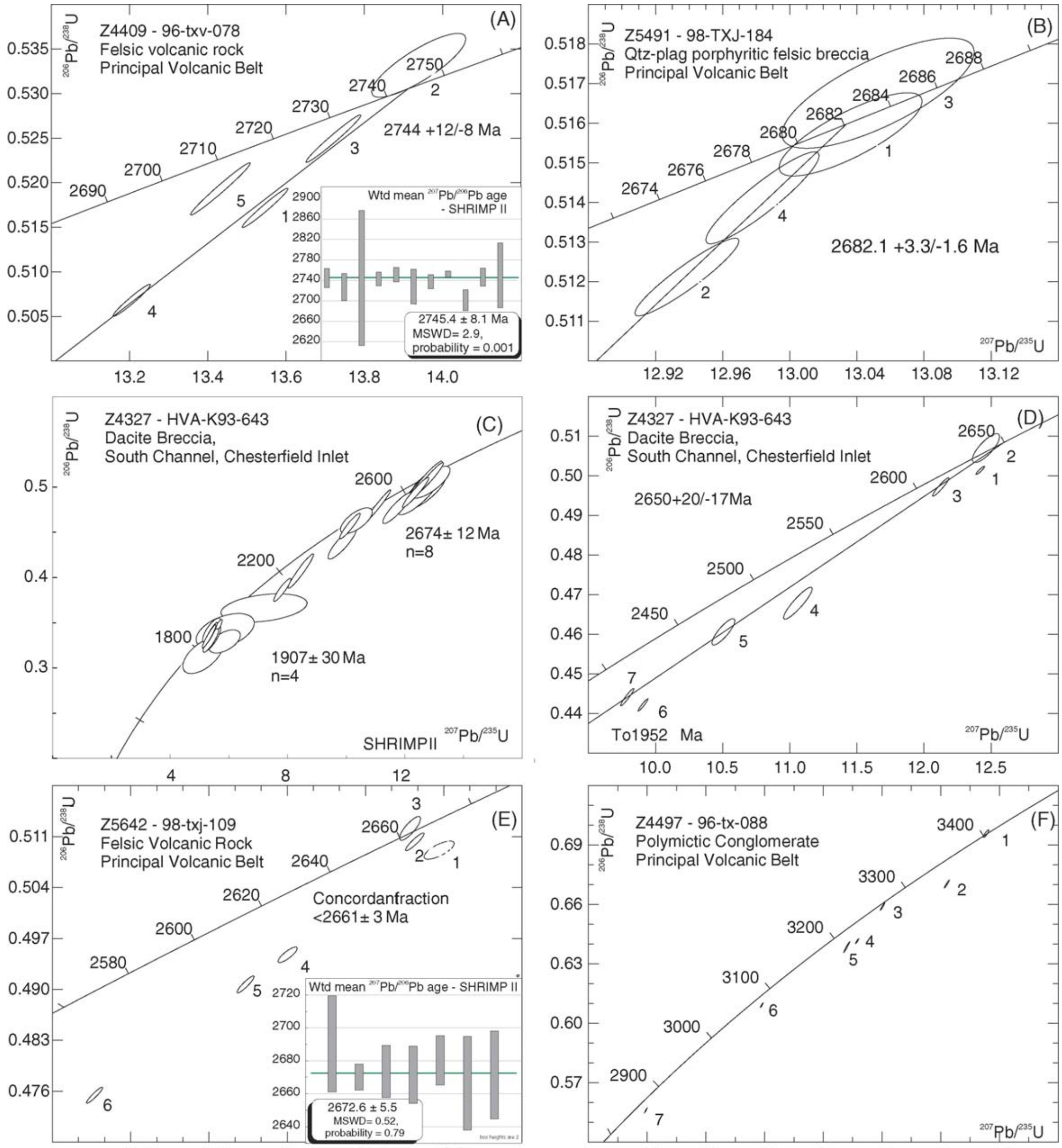

Fig. 5. U–Pb concordia diagram for supracrustal rocks, MacQuoid supracrustal belt.

Sample Z4327 is from a dacite breccia from the southwest-trending volcanic belt exposed along the South Channel of Chesterfield Inlet (Fig. 2). The volcanic belt consists of intermediate and subordinate mafic volcanic rocks with a high proportion of interbedded lithic tuffs (Sanborn-Barrie, 1999). Zircon consists of prismatic, euhedral grains that yield a broad range of discordant ages (Fig. 5D). The trend of the ID-TIMS data array extends towards a lower intercept defined by two concordant titanite analyses at 1.90 Ga (Table 1). The titanites are interpreted to date Paleoproterozoic metamorphism in the area, and the zircon data array is consistent with a significant component of Pb-loss and/or recrystallization of zircon at that time. Ion probe analyses document a wider array of ages between 1.9 and 2.7 Ga that correlate with Th/U ratio (Fig. 5C). The age array is interpreted to indicate variable recrystallization of the zircon during ∼1.90 Ga metamorphism, with the recrystallized zircon domains characterized by low Th and Th/U ratios (Table 2). The weighted mean age

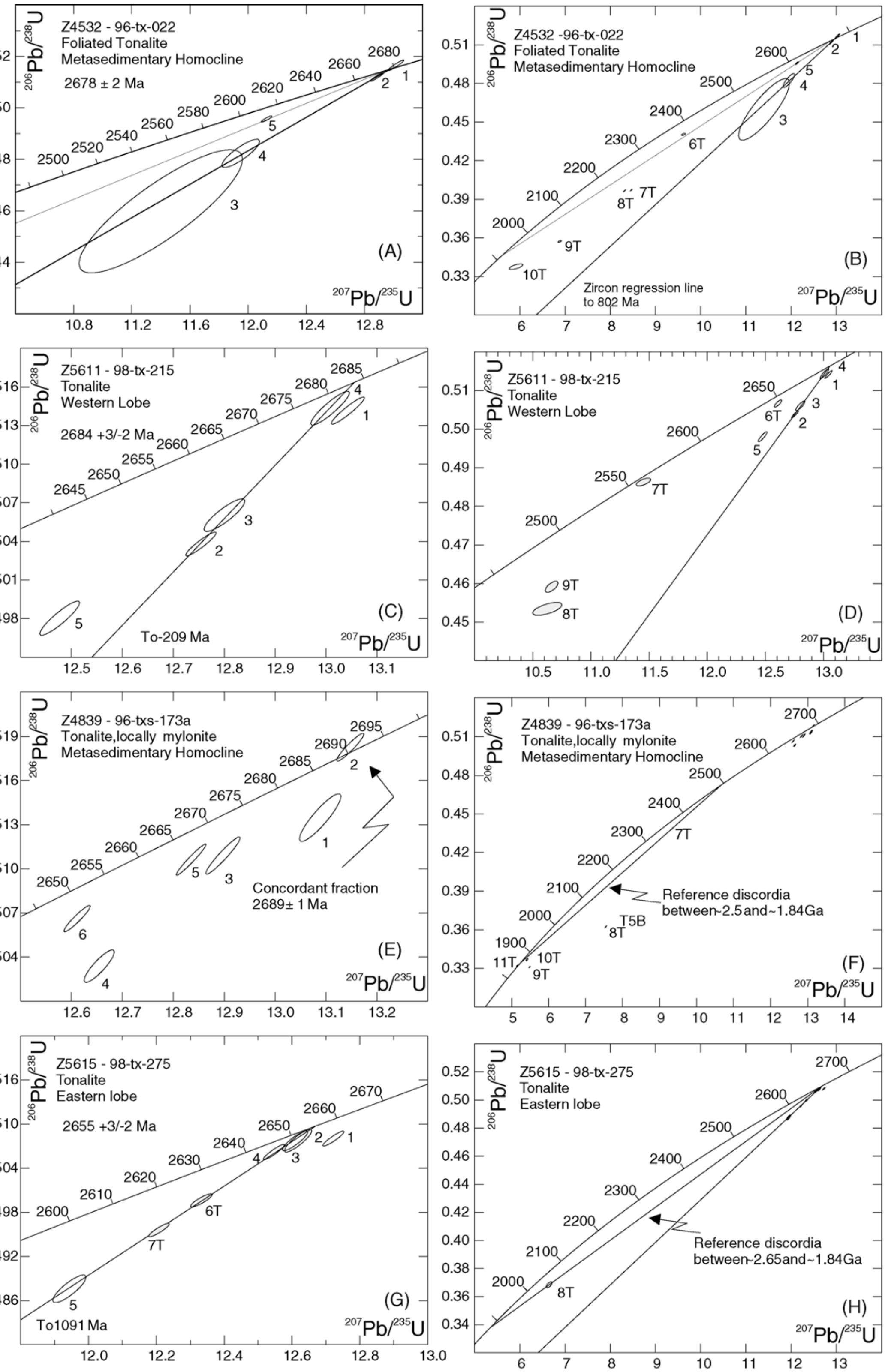

Fig. 6. U–Pb concordia diagrams for plutonic rocks from the MacQuoid homocline.

for the zircon with Th/U ratios >0.3, interpreted to be least affected by the recrystallization, is 2674 ± 12 Ma (MSWD = 1.7; POF = 0.11) a date interpreted as the crystallization age of the volcanic rock. The youngest zircon ages at ∼1.90 Ga are consistent with the metamorphic age recorded by titanite (Table 3).

Sample Z4497 is from a 3 to 5 m thick, polymictic conglomerate unit interlayered with mafic volcanic rocks on the north side of the principal volcanic belt (Fig. 2). The conglomerate contains a range of clast types including foliated granitoids and mafic volcanic fragments of uncertain origin. A sample of sand to small pebble-sized matrix material, excluding the larger clasts, was selected for analyses. Zircon exhibit a range of morphologies from sharp prisms to rounded grains, and have a range of Mesoarchean ages between 2890 and 3400 Ma (Fig. 5F). There is no obvious correlation of age with the degree of rounding. Mesoarchean crust was an important source to this conglomerate, however, its depositional age and primary relationship to the adjacent volcanic rocks remains unresolved.

5.3. Geochronology of intrusive rocks, MacQuoid supracrustal belt

Six samples of intrusive rocks were collected from the MacQuoid supracrustal belt to evaluate the timing of plutonism and its relationship to the regional transposition fabric. Two principal Archean plutonic events are documented: (i) 2685–2655 Ma tonalites, which include gneissic and plutonic rocks in the metasedimentary homocline and principal volcanic belt and (ii) younger, ∼2610 Ma granitic intrusions, represented by the augen granite. All of these plutonic rocks pre-date the regional transposition fabric, and thus provide maximum ages for its development. Data for one sample of a Proterozoic granite is also reported.

Sample Z4532 is from a strongly foliated tonalite layer within the metasedimentary homocline (Fig. 2). The unit contains layer-parallel granitic veins that were carefully avoided during sampling. The tonalite intruded the supracrustal rocks in the area and was subsequently deformed by the regional transposition fabric. It provides a minimum age for deposition of the sedimentary rocks, and a maximum age for the regional transposition fabric. Zircon consists of euhedral prismatic grains. Fraction 1 yields a concordant date of 2678 ± 2 Ma, which together with three variably discordant zircon fractions (2–4) define a regression line with an upper intercept age of 2678 ± 2 Ma (MSWD = 0.46; Fig. 6A), interpreted as the crystallization age of the tonalite. One discordant fraction (#5) has a younger apparent age of 2630 Ma, and plots on a reference discordia between 1.9 and 2.68 Ga, interpreted to result from a Paleoproterozoic disturbance for this fraction, similar to that observed in sample Z4327. Paleoproterozoic effects are also evident in the discordant titanite analyses. In general, the darkest brown titanite is oldest (e.g. 6T), and colourless varieties are youngest.

Sample Z5611 is from the western-most, lobate tonalite pluton located just beneath the eastern branch of the principal volcanic belt (Fig. 2). The pluton intruded the adjacent volcanic units, and the regional transposition fabric wraps around it. Zircon is dominated by euhedral, prismatic grains, with a subordinate population of rounded, ovoid grains. A small subset of prismatic zircon had observable cores, which were excluded as best as possible from analyses. Three of four fractions of prismatic zircon define a regression with an upper intercept age of 2684 + 3/−2 Ma, taken as the crystallization age (Table 3; Fig. 6C). Fraction 5, the most discordant result, comprises elongate, thin prisms, and the analysis plots to the left of the discordia line indicating an additional component of Pb-loss. This is consistent with the high surface area to volume ratio determined by grain morphology and less effective abrasion prior to analyses. The ovoid, rounded grains (fraction1) yield an older $^{207}Pb/^{206}Pb$ date of 2689 Ma, interpreted to reflect the inherited component observed as cores in many grains. Titanite ranges in colour from dark brown to pale brown, with the darker grains having older, less discordant ages. Three of the four analyses have ages in the range of 2540–2566, including analysis 7T, which is only 0.5% discordant (Fig. 6D). The titanite dates may indicate partial resetting during the ∼2.50–2.55 Ga metamorphism documented for this area (Stern and Berman, 2001; Berman et al., 2000).

Sample Z4839 is from a locally mylonitic, steeply dipping, dip-lineated tonalite in the western part of the metasedimentary homocline (Fig. 2). The mylonite zones, in part, deformed intrusive mafic sheets correlated with the ∼2.19 Ga MacQuoid dykes, and are therefore interpreted to include a component of Proterozoic (post 2.19 Ga) deformation. Zircon occurs as euhedral, prismatic grains, many of which exhibit overgrowths. The zircon fractions yield $^{207}Pb/^{206}Pb$ dates between 2697 and 2658 Ma (Fig. 6E), with no simple age interpretation. A concordant result at 2689 ± 1.4 Ma provides a maximum age for the tonalite. Five titanite analyses show a large range in $^{207}Pb/^{206}Pb$ dates from 2396 to 1841 Ma (Fig. 6F). Fractions with older ages consist of darker brown titanite, whereas the younger dates are recorded by very pale brown titanite. The youngest concordant titanite (11T) at 1841 Ma could reflect growth or recrystallization related to late movement along the mylonite zone. Titanite fraction 7T lies on a reference discordia between the ∼1.84 Ga titanite and an upper intercept date of ∼2.50 Ga, perhaps indicating the effect of the regional 2.55–2.50 Ga metamorphism (Stern and Berman, 2001).

Sample Z5615 is a tonalite that forms the eastern lobate pluton between the eastern branch of the principal volcanic belt and the metasedimentary homocline (Fig. 2). Similar to Z5611, the transposition fabric wraps around the pluton. Zircon is dominated by colourless, subhedral, stubby prisms. Regression of four of the five analyses (#2–5) yields an upper intercept age of 2655 + 3/−2 Ma, interpreted as the crystallization age (Fig. 6G). One fraction (#1), with a significantly older apparent age of 2668 Ma, is interpreted to contain an inherited component. The 2655 Ma age is significantly younger than the other dated tonalites in the area, and places a maximum age on development of the enveloping regional transposition fabric. It is, however, similar to ages for some of the volcanic rocks in the volcanic belts to the north. Two fractions of clear brown to light brown titanite plot on the discordia line defined by the zircon analyses, suggesting a magmatic origin. Clear colourless titanite (8T) is significantly younger and plots on a reference isochron between ∼1.87 and 2.55 Ga (Fig. 6H), suggesting some recrystallization during the Paleoproterozoic.

Sample Z4527 is from the large, poorly exposed, augen granite along the northern margin of the principal volcanic belt (Fig. 2). The pluton contains a heterogeneously developed foliation that is parallel to the regional trends of the main transposition fabric within the supracrustal rocks, and thus provides a maximum age for the transposition fabric. Zircon consists of subhedral, prismatic grains of poor optical clarity. Four of seven, multi-grain analyses, including one concordant result define a regression line with an upper intercept age of 2610 + 10/−9 Ma (Fig. 7A; Table 3); interpreted as the crystallization age of the pluton. Three fractions (1, 2 and 6) plot to the right of this discordia and were excluded from the regression. These fractions may contain an inherited component and/or have greater recent Pb-loss.

Sample Z4685 is a homogeneous, massive biotite granite pluton or stock that cut the north margin of the principal volcanic belt (Fig. 2). Based on field characteristics the pluton is correlated with regional ∼1.83 Ga plutons (Tella et al., 1997a,b). Relationships to the surrounding host rocks are not exposed. Zircon recovery was poor. A single, multi-grain analysis of doubly terminated, small prisms produced a date of 1827 ± 2.4 Ma (Fig. 7B), interpreted as the intrusion age. Two analyses

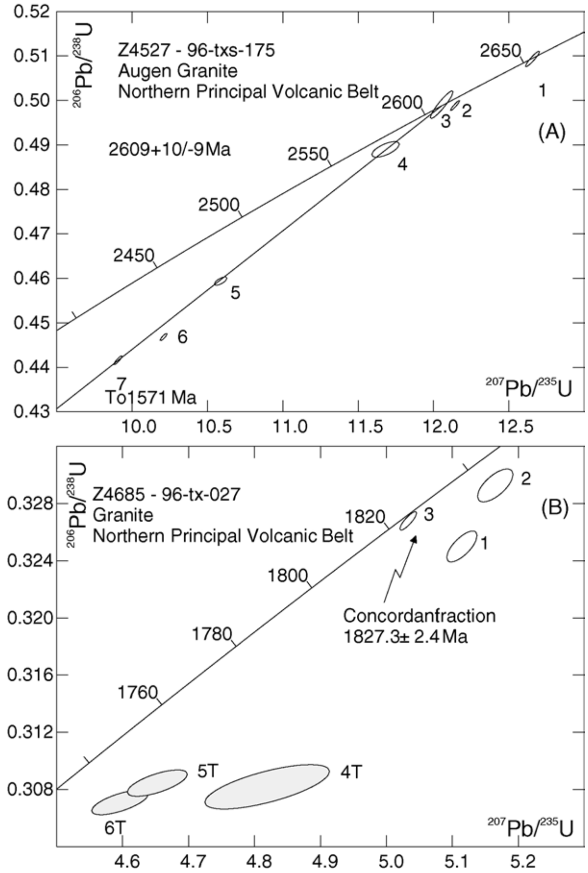

Fig. 7. U–Pb concordia diagram sample Z4527 and Z4685.

of larger grains with thin overgrowths yielded older discordant ages and are interpreted to include an inherited component. Titanite yields younger discordant dates.

6. Cross Bay plutonic complex

The Cross Bay plutonic complex is composed of orthogneiss and plutonic rocks north and east of the metasedimentary homocline and the volcanic belts, respectively (Hanmer et al., 1999a, 2004; CBC in Fig. 2). The complex is predominantly composed of tonalite to diorite in its central part with granitic plutons in the eastern and western sectors. The tonalites are typically gneissic and similar in appearance to those within the MacQuoid supracrustal belt (cf. Figs. 3 and 4). They are commonly intruded by pervasive, 5 cm to 50 m thick, semi-concordant sheets of biotite monzogranite to granodiorite, which show a wide range of deformation states. East of the Cross Bay fault (CBF, Fig. 2), the tonalite intrudes map-scale panels of diorite, gabbro and amphibolite. In the western part of the complex, variably foliated granite, the South Channel granite, intrudes the tonalite gneisses. Its relationship to early fabrics in its host rocks is described below.

6.1. Structure in the Cross Bay plutonic complex

The structure of the Cross Bay plutonic complex is described in detail by Hanmer et al., 2006). Structural elements within the complex include a penetrative, layer-parallel foliation, an extension lineation (~0–20°), and open to tight folds of the foliation (Hanmer et al., 1999b, 2006). As described by Hanmer et al. (2006) similarly oriented structures can be demonstrated to have formed in the Neoarchean and Paleoproterozoic, and it is difficult to resolve fabric elements based solely on geometrical arguments.

West of Cross Bay, the foliation is generally steep and north–south-trending. In the tonalite gneisses, it is locally deformed about isolated, open to tight, metre- to map-scale, upright, south-plunging folds and coaxial with a pervasive extension lineation (e.g. #7 Fig. 2). South and east of Cross Bay, the foliation in the tonalitic and dioritic gneisses is deformed about two sets of upright structures: (i) moderate to tight, east–northeast-plunging folds and (ii) open, south-plunging folds (#8 and #9 Fig. 2, respectively). The second set is coaxial to an extension lineation that is well developed in the gneisses. Ryan et al. (1999, 2000) correlated the first set of these structures with the east–northeast-plunging folds of the transposition fabric in the principal volcanic belt, interpreted as Proterozoic in age.

The MacQuoid supracrustal belt and the Cross Bay plutonic complex are separated by the Big Lake shear zone (Fig. 2), a steeply north-dipping belt of porphyroclastic straight gneisses and ribbon mylonites, up to 2 km thick (see Hanmer et al., 1999b, 2006; Ryan et al., 2000 for details). The shear zone was active under amphibolite to granulite-facies conditions at ~2.50 Ga (Ryan et al., 2000), and is interpreted as a thrust fault putting the Cross Bay complex over the supracrustal belt. The shear zone post-dates the development of the main transposition fabric in the supracrustal belt (Hanmer et al., 2006).

In the western part of the Cross Bay plutonic complex, the South Channel granite (#10, Fig. 2) interdigitates semi-concordantly with respect to the host tonalite gneiss, but is locally discordant to the wallrock foliation. At the outcrop scale, moderately foliated granite contains strongly foliated and lineated, concordant rafts of tonalite. These observations indicate that the granite was emplaced and deformed after the development of an early L/S fabric in the tonalite gneiss. The granite (Z5687) was sampled to provide a minimum age for the timing of the early deformation of the tonalitic wallrocks.

Smaller-scale granitic veins (<1 m) also intruded the tonalitic gneiss, but demonstrate variable relationships to the south-plunging folds of the foliation in the tonalite. Some veins are deformed by the south-plunging folds, and others cut the same folds. Accordingly, samples of the host tonalite and a granitic vein were sampled in order to date their magmatic crystallization and bracket the age of the south-plunging folds in the gneisses of the western part of the Cross Bay plutonic complex (Z5641 and Z5616).

West of Cross Bay, the plutonic complex was cut by metamorphosed dykes interpreted to be part of the MacQuoid swarm. Garnet-clinopyroxene-bearing assemblages record deep-crustal metamorphic conditions of 700–750 °C at 1.1–1.3 GPa, comparable to those obtained from dykes in the metasedimentary homocline, and presumably similar in age (~1.90 Ga; Berman et al., 2000). The dykes cross-cut and post-dated the wall-rock foliation and were subsequently folded with axial plane traces parallel to those of the south-plunging folds described above (Hanmer et al., 1999b, 2006). Although dykes suitable for dating were not found, correlation with equivalent dykes in the metasedimentary homocline suggests a maximum age of ~2.19 Ga for deep-crustal tectonothermal reworking of the Cross Bay plutonic complex.

The eastern parts of the plutonic complex are intruded by plutons and map-scale sheets of biotite ± fluorite monzogranite and granodiorite similar to those in the homocline (#9 and #11 Fig. 2). These intrusions are homogeneous, medium grained, equigranular and moderately foliated to isotropic, with well preserved igneous textures. The granites are correlated with the 1840–1810 Ma Hudson granites (Peterson et al., 2002; see also van Breemen et al., 2005). Some plutons are composite, ranging from monzogranite, through monzonite, to phlogopite gabbro, and commonly show evidence for magma commingling (Sandeman et al., 2000b). These granitic rocks intruded the tonalitic and dioritic wallrocks late in the regional deformation history and record variable strain states. In particular, map-scale granodiorite sheets at the north end of Big Point peninsula (#9 in Fig. 2) were openly folded about south-plunging folds with a coaxial extension lineation. Locally, at outcrop scale, non-deformed veins of granodiorite cut strongly deformed sheets of the same composition that were previously injected into tonalite gneiss (Fig. 9). Samples of both deformed and non-deformed granitic sheets were taken to determine magmatic crystallization ages and constrain the timing of the end of the youngest regional deformation in the eastern part of the plutonic complex.

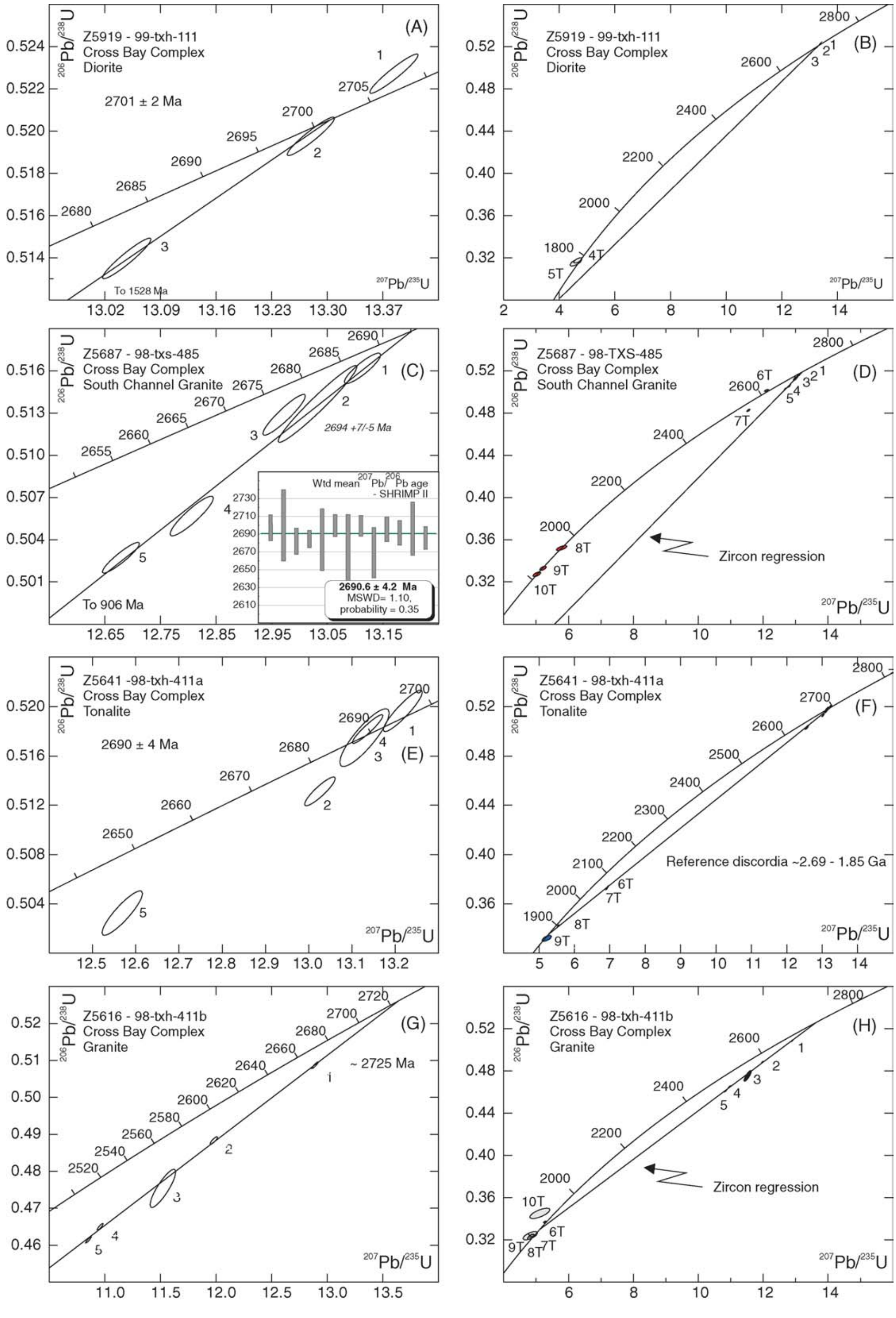

Fig. 8. U–Pb concordia diagram for rocks from the Cross Bay plutonic complex.

The northern part of the monzogranite pluton in Big Point peninsula (#11 in Fig. 2) contains a body of well foliated, biotite-hornblende monzonite that shows commingling textures similar to those in the monzogranites. It was sampled in order to date its magmatic crystallization and determine whether it represents an early member of the Paleoproterozoic plutonic suite, or part of a significantly older suite (Z5915).

7. Geochronology of the Cross Bay plutonic complex

Sample Z5919 is a hornblende diorite collected as representative of the older intrusive component of the Cross Bay plutonic complex (Fig. 2). Zircon occurs as euhedral prismatic crystals. Three multi-grain analyses define a regression line with an upper intercept age of 2701 ± 2 Ma, pinned by a single concordant result (Fig. 8A; Table 3). This is interpreted as the crystallization age of the diorite. Titanite yields younger dates with two analyses overlapping concordia at ∼1.77 Ga, the weighted average of the $^{206}Pb/^{238}U$ ages (Fig. 8B).

Sample Z5687 is from the variably foliated, K-feldspar porphyritic South Channel granite. As described above, some fabric development in the Cross Bay plutonic complex pre-dated intrusion of this pluton. The well-developed augen textures and local gneissosity within this pluton indicate that the more significant fabric development in the Cross Bay complex occurred after its intrusion.

Zircon consists of prismatic to stubby prisms of relatively simple morphology. Regression of four of the five analyses yields a discordia line with a poor probability of fit and an upper intercept age of 2694 + 7/−5 Ma (Fig. 8C; Table 3). Ion microprobe analyses of thirteen grains yield a more precise, weighted mean age of 2691.6 ± 4.2 Ma (MSWD = 1.1). The ion probe result is identical within error to the interpreted age based on the ID-TIMS data, and is interpreted as the crystallization age of the pluton. Two analyses of anhedral, dark brown titanite have concordant to slightly discordant ages of 2607–2592 Ma, indicating titanite growth or resetting at, or soon after ∼2.60 Ga (Fig. 8D). Younger, colourless to light brown titanite, indicate a period of new titanite growth/recrystallization during the Paleoproterozoic at ∼1.82–1.84 Ga.

Sample Z5641 is a foliated tonalite, characteristic of the dominant lithology in the Cross Bay plutonic complex. Zircons comprise large, prismatic to tabular colourless prisms. Four of the five analyses have $^{207}Pb/^{206}Pb$ ages between 2689 and 2694 (Fig. 8E), with a weighted mean age of 2690 ± 4 Ma, taken as the best estimate of the crystallization age of the rock (Table 3). The fifth fraction consisted of flat, tabular grains, more difficult to abrade, and yielded a more discordant date of 2663 Ma. Titanite analyses are all much younger than the crystallization age and exhibit the same pattern as observed in other samples from the area (Fig. 8F). Brown titanites preserve slightly older ages with paler titanite having more concordant ages at ∼1.85 Ga. The data plot along a reference discordia between the crystallization age and ∼1.85 Ga, indicating recrystallization during the latter thermal event.

Sample Z5616 is from a narrow (<1 m) granitoid vein that cross-cut the foliation developed in sample Z5641, and was in turn openly folded about the south-plunging fold set. Zircon analyses in this rock are discordant and do not define a statistically meaningful discordia (Fig. 8G). The data plot along a discordia array with intercepts at 2725 and 1836 Ma. The upper intercept date cannot be interpreted as the crystallization age of this granitoid as it demonstrably intruded the 2690 ± 4 Ma tonalite (Z5641). The zircon within this rock is dominantly inherited, and the age of magmatic crystallization cannot be interpreted. Titanite yields reversely discordant Paleoproterozoic ages (Fig. 8G and H). Reverse discordance may be due to incorporation of a relatively radiogenic Pb during recrystallization (e.g. Romer, 2001).

Samples Z5613 and Z5614 were collected from the north end of Big Point peninsula (Fig. 2) to constrain the timing of the last major regional deformation in the eastern part of the Cross Bay plutonic complex. Z5613 is a deformed granite dyke that intruded a foliated tonalite host (Fig. 9). Sample Z5614 is a cross-cutting, non-

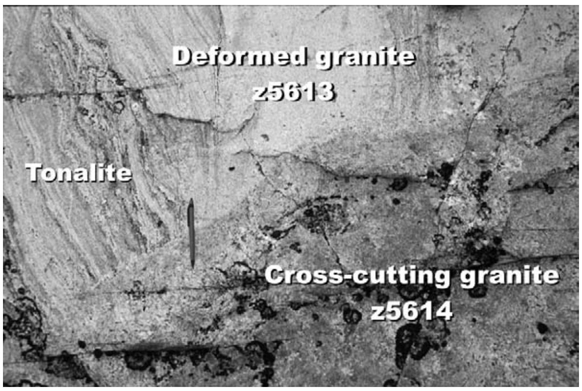

Fig. 9. Photograph of intrusive relationships, northeastern Cross Bay plutonic complex. Sample Z5613 was taken from a representative generation of granite veins that cut an earlier foliation in the host tonalite (vertically oriented in photograph), but are themselves folded and foliated. Sample Z5614 comes from a cross-cutting non-deformed granite dyke.

deformed dyke (Fig. 9). Collectively the two samples are interpreted to bracket the final increments of strain in this area.

Zircon in Z5613 is dominantly prismatic to tabular. Cores are observed in some grains, and these were not selected for analyses. Clear overgrowth tips separated from prisms with visible cores yield the oldest ages (1–4; Table 1), indicating that core or xenocrystic material was not completely excluded in these selections. Prisms without visible cores (6–8) and one fraction of an overgrowth tip (9) yield an upper intercept regression age of 1828 + 10/−7 Ma pinned by a concordant grain (#6; Fig. 10A). This is interpreted as the crystallization age of the granite. Two generations of titanite occur in the sample, clear brown grains and colourless to pale brown grains. The former are reversely discordant with $^{207}Pb/^{206}Pb$ ages of ∼1750 Ma (Fig. 10B). Colourless to pale brown titanite are younger with an age of ∼1725 Ma (13T).

Zircon in sample Z5614 consists dominantly of anhedral, colourless fragments. Two morphological subtypes were identified: blocky and flat. Two analyses of the blocky fragments (2 and 3), and one of the flat fragments (1) yield discordant $^{207}Pb/^{206}Pb$ dates between 1816 and 1814 Ma. One of the flat fragments (#4) is concordant at 1806 ± 2.6 Ma, significantly younger than the other analyses (Fig. 10C). Four multi-grain analyses of brown titanite yield discordant results and an upper intercept age of 1807 ± 2 Ma (forced to zero lower intercept). This age is identical to concordant zircon fraction #4, and a combined zircon and titanite regression yields an upper intercept of 1807 + 3/−2 Ma interpreted as the best age estimate for the granite. The older ages of the other three zircon analyses are interpreted to indicate an inherited component in those fractions. Deformation in this outcrop occurred prior to 1807 + 3/−2 Ma.

Sample Z5915 is a foliated hornblende-biotite monzonite from the east side of the Big Point peninsula (Fig. 2). The pluton exhibits an intimate co-magmatic association with lamprophyre intrusions. The weighted average of four prismatic zircon analyses (1–4) yields an age of 1830.3 ± 1.7 Ma (MSWD = 0.94; Fig. 10D), and is interpreted to be the age of the intrusion. Titanite yield apparent ages between 1780 and 1824 Ma (5T–7T).

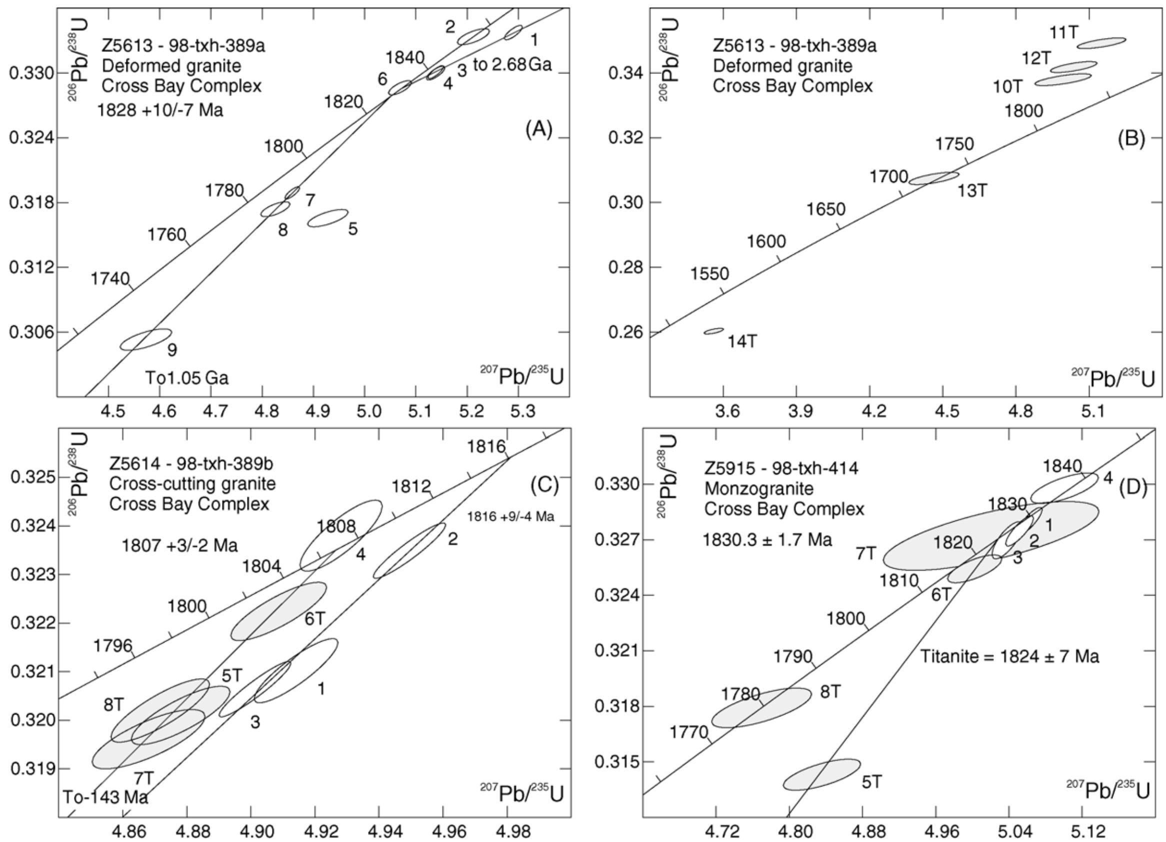

Fig. 10. U–Pb concordia diagram for samples of Proterozoic intrusive rocks.

Three titanite analyses yield an upper intercept age of 1824 ± 7 Ma (Fig. 10D), within error of the zircon age. A fourth analysis of pale titanite (8T) yields a younger concordant date of 1780 Ma.

8. Discussion

8.1. Timing of Neoarchean crust formation

Volcanic and plutonic rocks in the MacQuoid supracrustal belt developed over a time period from <2.74 to 2.66 Ga, with the majority of the rocks formed between 2.69 and 2.67 Ga (Fig. 11). Plutonic rocks of the Cross Bay plutonic complex, with ages of 2.70–2.69 Ga are slightly older than the majority of igneous rocks in the MacQuoid supracrustal belt. Additionally, they locally contain inheritance of older 2725 Ma zircon (sample Z5616), and Nd isotopic data indicate involvement of older, Mesoarchean crustal protoliths in their generation (Sandeman et al., 2000a). The Nd isotopic compositions contrast with the data from the supracrustal belt that indicate more juvenile compositions. The slight difference in age, the presence of an early, pre 2694 Ma tectonic fabric, and the isotopic evidence for different crustal sources argue for a separate origin of the Cross Bay plutonic complex, and highlight the potential for the Big Lake shear zone to represent a significant regional structure that juxtaposed these different blocks (Ryan et al., 2000).

The extensive deformation and transposition of the supracrustal belt obscured primary stratigraphic relationships. The development of a stratigraphic model for the belt is precluded. Although the geochronological data suggest that as many as three volcanic successions with distinct ages may be present within the belt (<2.74, 2.69–2.68 and 2.67 Ga), the primary stratigraphic relationship between the volcanic successions, and to the spatially associated sedimentary units is not known. The volcanic ages are dominantly younger than the 2.74–2.71 Ga ages of volcanic belt development in the Rae (e.g. Woodburn and Prince Albert Group, Davis and Zaleski, 1998; Skulski et al., 2003).

The full extent and relationships between the different supracrustal successions cannot be defined. Some metasedimentary rocks within the homocline have a minimum depositional age of 2678 ± 2 Ma, provided by the intrusive age of sample Z4532. Although no upper limit is determined, these rocks may be broadly similar in age to the ca. 2.68 Ga volcanic successions. The relationship and distribution of the younger succession of volcanic rocks and temporally associated tonalite dated at ∼2672–2655 Ma remains unknown. Similarly, the relationship of the mafic volcanic sequences of the principal volcanic belt to the intercalated polymictic conglomer-

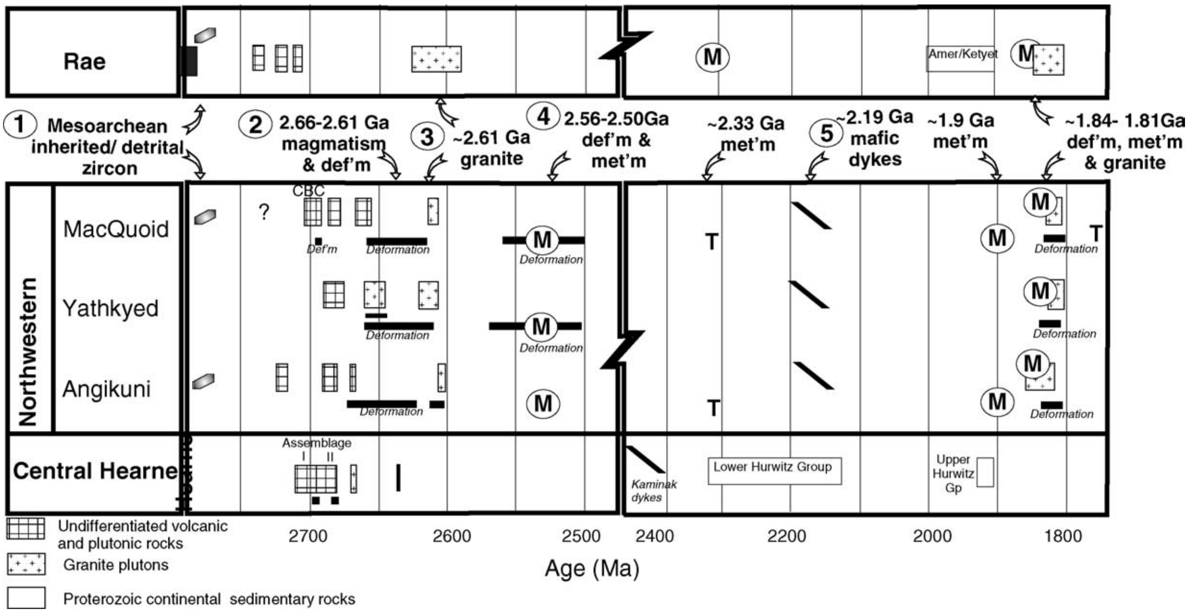

Fig. 11. Summary of principal tectono-metamorphic events in different regions of the SE Rae, and northwestern and central Hearne subdomains. Information from Rae pertains mostly to Woodburn Lake area north of Baker Lake (Davis and Zaleski, 1998; Zaleski et al., 2001) (M, metamorphic event and T, titanite age). Data sources as referenced in text. The key tectonic elements of the northwestern Hearne subdomain are highlighted and numbered 1–5.

ate with Mesoarchean detrital zircon remains uncertain. If the intercalation was primary, then the volcanic rocks formed in proximity to a source containing, and possibly dominated by older Mesoarchean crust. Potential basement rocks of this age are not known in the local area but are documented in quartzite from the Meadowbank area in the Rae province (Davis and Zaleski, 1998). However, the possibility that the conglomerate is younger (or older for that matter) and structurally imbricated with the volcanic rocks cannot be entirely eliminated.

The volcanism in the MacQuoid supracrustal belt is predominantly younger than the main period of volcanic belt development in the better preserved central Hearne supracrustal belt to the south (2711–2691 Ma; assemblage I), but it does overlap with the younger, volcano-plutonic and sedimentary sequences (2685–2680 Ma; assemblage II; Fig. 11; Hanmer et al., 2004; Davis et al., 2004). Therefore, the belts are in part contemporaneous (Fig. 11). However, volcanism and tonalite plutonism continued to younger ages in the MacQuoid supracrustal belt as evidenced by the 2672–2655 Ma volcanic and tonalite rocks. In the central Hearne this time period post-dated intrusion of the youngest, post-kinematic granites dated at 2667 Ma (Davis et al., 2004). Magmatic rocks of this age are well represented in the other parts of the northwestern Hearne subdomain in the Yathkyed supracrustal belt (Fig. 1; MacLachlan et al., 2005a). Tella and Roddick (1995) reported an age of 2661 ± 3 Ma for fine-grained felsic rocks from Rankin Inlet (Fig. 1).

8.2. Timing of Neoarchean regional deformation

The earliest deformation structures recognized in the area are the pre 2692 Ma fabrics within the western Cross Bay plutonic complex. The early fabric in the Cross Bay complex pre-dates the formation of most of the rocks in the underlying MacQuoid supracrustal belt, with the possible exception of the <2745 Ma volcanic unit. The age relationships are consistent with the Cross Bay plutonic complex preserving a different tectonic history and being in fault contact with the younger rocks of the MacQuoid supracrustal belt along the Big Lake shear zone (Ryan et al., 2000; Hanmer et al., 2006).

Estimates of the maximum and minimum ages for the early, pre-transposition fabrics preserved in the principal volcanic belt (Ryan et al., 1999) are poorly constrained. The fabrics must post-date the 2682 Ma volcanic rocks and 2655 Ma eastern tonalite dome, and pre-date the syn-transposition, metamorphic monazite age of 2.55 Ga reported by Stern and Berman (2001). The relationship of the intervening 2610 Ma augen granite (Z4527) to the pre-transposition fabrics is not observed, but the fact that it is foliated means some fabric development occurred syn or post 2610 Ma. Deformation between 2.66 and 2.61 Ga is well documented along the Tyrrel and Nowyak shear zones in the Yathkyed supracrustal belt, southwest of the MacQuoid belt (Fig. 2; MacLachlan and Relf, 2000; MacLachlan et al., 2000, 2005a) and is interpreted to be related to thrust nappe tectonics at 2.66–2.64 Ga (MacLachlan et al., 2005a). Deformation at 2.68–2.61 Ga is also documented in the Angikuni Lake area (Aspler et al., 1999). Although speculative, the early fabric development at MacQuoid may be correlative with Neoarchean fabrics elsewhere in the northwestern Hearne subdomain.

The maximum age for development of the regional transposition fabric in the MacQuoid supracrustal belt is constrained by the 2655 Ma intrusive age of sample Z5615, and a minimum age is provided by the 2.50 Ga Big Lake shear zone, which was penecontemporaneous with, but truncated, the transposition fabric. The 2.66–2.50 Ga age constraint for the development of the transposition fabric is consistent with previous interpretations of 2.56–2.54 Ga fabrics in the South Channel of Chesterfield Inlet along the northern extension of the MacQuoid belt (Sanborn-Barrie et al., 2001), within the southern part of the Uvauk complex (∼2.62–2.51 Ga; Mills et al., 2000), and syn-kinematic metamorphic ages of ∼2.56–2.50 Ga for rocks of the metasedimentary homocline (Stern and Berman, 2001; Berman et al., 2000). A similar age of deformation and amphibolite-facies metamorphism is also locally documented in the Yathkyed and Angikuni supracrustal belts to the southwest (Fig. 2; MacLachlan et al., 2005a; Berman et al., 2002a).

The timing of Neoarchean structures in the Cross Bay plutonic complex is poorly known. The dominant foliation developed after 2690 ± 4 Ma, the age of the youngest intrusive phase that contains the fabric, and prior to intrusion of the mafic dykes interpreted to be correlative with the 2190 Ma MacQuoid swarm. The foliation in the CBC is interpreted to have formed prior to 2500 Ma because the foliation is deformed about folds that increase in intensity towards the Big Lake shear zone. This allows that the fabrics developed at the same time as those in the supracrustal belt. The relationship of the pre 2692 Ma fabrics that were cut by the South Channel granite to the post 2690 Ma regional fabric within the Cross Bay plutonic complex is not known, but it is likely that the older fabric is not the dominant regional fabric in the complex. It is clear that multiple coplanar fabrics of different age occur within the complex.

8.3. Paleoproterozoic tectono-thermal reworking

The area experienced variable but extensive reworking at several times in the Paleoproterozoic. In contrast to the Neoarchean structures that are prominent fabric-forming events, the Paleoproterozoic deformation is characterized mostly by folding (from decimeter scale to map-scale) and stretching lineation development. Both the metasedimentary homocline of the MacQuoid supracrustal belt, and the western segment of the Big Lake shear zone, yield evidence for a ∼1900 Ma, static, deep-crustal (∼1.0 GPa) metamorphic event recorded by post-foliation growth of garnet in metasedimentary rocks, as well as in the ∼2190 Ma MacQuoid dykes (Berman et al., 2000; Ryan et al., 2000). The metamorphism is not interpreted to be associated with fabric development and is discussed in more detail by Berman et al. (2000). Little direct evidence for this metamorphism is preserved in the samples from this study with the notable exception of the 1900 Ma titanite and recrystallized zircon ages from the volcanic breccia on the South Channel, in the northern part of the study area.

Most of the area, including both the Cross Bay plutonic complex and MacQuoid supracrustal belt, was thermally and locally tectonically reworked during ∼1830–1780 Ma metamorphism. In the eastern part of the supracrustal belt the reworking was associated with the emplacement of granitic plutons (#12, Fig. 2), and in the western part it was recorded by the deformation of MacQuoid dykes. The timing of this deformation is not tightly constrained although granites with intrusive ages of ∼1840–1830 Ma preserve some of these fabrics, and crystallization or recrystallization of titanite at 1840 Ma in a small mylonite zone indicate that it was most likely part of the widespread Hudsonian event.

The Cross Bay plutonic complex was affected by post-MacQuoid dyke folding that reworked older, coaxial structures in the gneisses, as well as intrusive rocks as young as 1816 Ma. In the northeastern part of the complex, a minimum age for these fabrics is given by the 1807 Ma age of a post-kinematic granite intrusion (Z5614). In the same outcrop a slightly older, 1816 Ma intrusive sheet contains a penetrative fabric, thus bracketing the last increment of strain for the folding event to between 1816 and 1807 Ma. These age estimates for deformation are comparable to those from the homocline and suggest that both domains experienced the 1.84–1.81 Ga deformation.

Titanite ages in a range of rock types within the MacQuoid supracrustal belt, indicate widespread, post 1900 Ma recrystallization or growth. Although commonly difficult to precisely determine because of mixing with older titanite and partial resetting, Paleoproterozic titanite ages fall into three time windows: ∼1.9, ∼1.84 and ∼1.78 Ga (Fig. 12). In samples that record multiple titanite ages, a clear correlation between age and composition can be demonstrated, with the Paleoprotoerozoic titanite analyses having higher Th/U ratios (Table 1). This eliminates diffusional Pb-loss as the dominant process to account for the Paleoprotoerozoic ages, and points to new titanite growth or recrystallization. The oldest 1.9 Ga titanite are only preserved in the northern part of the belt, immediately south of the high-pressure 1.90 Ga rocks of the Kramnituar complex (Sanborn-Barrie et al., 2001). Elsewhere in the belt, titanite recrystallization occurred at ∼1.84–1.82 Ga, contemporaneously with intrusion of the Hudsonian granites (van Breemen et al., 2005, this study) and local deformation. Titanite ages at ∼1.78 Ga cannot be associated with a specific regional tectonic event, although they may be related to elevated fluid and heat flow associated with brittle faulting that accompanied deposition of the lower Dubawnt Group in the Baker Lake area (Rainbird et al., 2003).

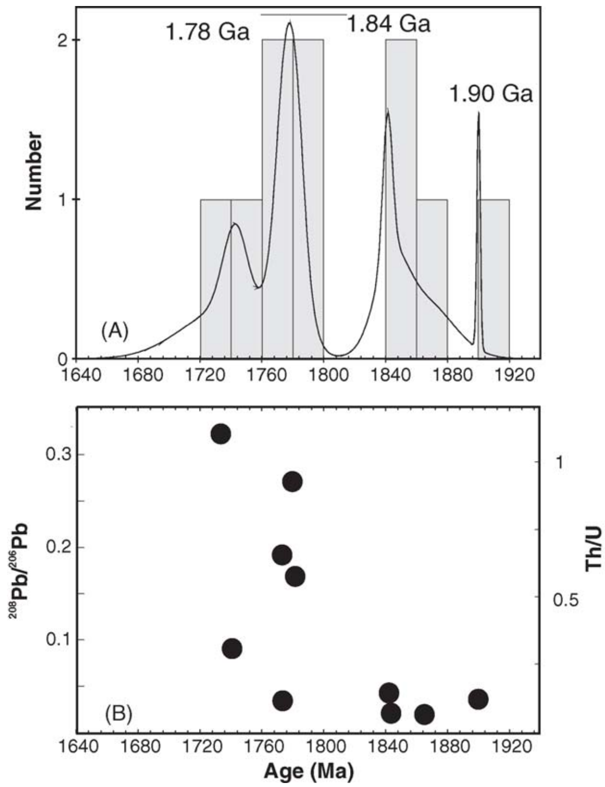

Fig. 12. (A) Cumulative probability plot and histogram of Paleoproterozoic titanite ages MacQuoid–Gibson Lakes area. (B) Plot of Th/U ratio (model) vs. interpreted age for younger titanite generations.

8.4. Tectonic elements of the northwestern Hearne subdomain

The new observations and data from the MacQuoid supracrustal belt and the Cross Bay plutonic complex contribute to defining the nature and tectonic history of the northwestern Hearne subdomain (e.g. Davis et al., 2000; Hanmer and Relf, 2000). The proposed subdomain occupies the northwestern part of the Hearne, paralleling the trace of the Snowbird zone (Fig. 1). The subdomain was initially proposed (Davis et al., 2000) based on: (1) dominantly Neoarchean crust formation between <2.74 and 2.66 Ga, with local evidence for interaction with Mesoarchean crust; (2) deformation in the interval between 2.66 and 2.61 Ga; (3) granite plutonism at 2.62–2.60 Ga; (4) regional metamorphism and deformation between 2.56 and 2.50 Ga and (5) distribution of the MacQuoid/Tulemalu mafic dyke swarm at 2.19 Ga, and absence of 2.45 Ga Kaminak dyke swarm (Fig. 11). Many parts of the area were subsequently thermally reworked at high-pressure at 1.9 Ga (Sanborn-Barrie et al., 2001; Berman et al., 2002a,b), and then deformed, metamorphosed and intruded by granite plutons at 1.84–1.81 Ga.

All of the features listed above, with the exception of the 2.66–2.61 Ga deformation, are documented in the MacQuoid area, and can be correlated with similar events at Yathkyed (MacLachlan et al., 2005a,b) and Angikuni (Aspler et al., 2000; Berman et al., 2002a) (Fig. 11). The nature and location of the boundaries to the northwestern Hearne subdomain are not precisely defined at this point (Fig. 1). This is largely due to extensive areas of no bedrock exposure along most of the southern boundary of the subdomain between MacQuoid and the central Hearne. In areas where the boundary may be observed it is expressed as younger, 1.83–1.81 Ga zones of deformation, plutonsim and metamorphism. For example, MacLachlan et al. (2005a,b) propose the Tyrell shear zone on the southeast side of the Yathkyed belt (Fig. 1) as the southeastern extent of the northwestern Hearne, but the structure presently juxtaposes 1.83 Ga metamorphsosed rocks of the central Hearne against less deformed rocks of the northwestern Hearne, and earlier relationships are very difficult to decipher.

The nature of the transition from the northwestern Hearne to the Rae is similarly poorly defined. At present it is taken as the geophysically defined trace of the Snowbird zone, however, it is not at all clear what the nature of this transition is. Although the geological characteristics of the northwestern Hearne subdomain can be clearly articulated, the tectonic significance in the context of the Rae–Hearne evolution remains unclear. The complex, polycyclic tectonic history of the northwestern Hearne subdomain as represented in the MacQuoid area, suggests that it may represent a collisional or accretionary orogenic zone developed along the southern margin of the Rae, or on a separate block between the Rae and central Hearne that was intermittently active over a prolonged period from 2.66 to 2.5 Ga. Although variably well constrained, the documentation of discrete tectonic events at 2.66–2.62, 2.56 and 2.50 Ga over a broad area of the northwestern Hearne suggests several Neoarchean orogenic events may have occurred over a 150 m.y. period. In general terms this is similar to observations in more recent accretionary orogens, such as the Appalachian, that preserve evidence of multiple events along a long-lived collisional margin (e.g. van Staal et al., 1998). The MacQuoid belt and the northwestern Hearne may represent a component of a long-lived, and complex continental margin setting between 2.66 and 2.50 Ga. Widespread 2.62–2.58 Ga granites within the northwestern Hearne and Rae may have developed in response to subduction along this margin. Owing to the extensive reworking of the zone during the Paleoproterozoic (1.9 and 1.84–1.81 Ga) it is not known if final amalgamation of the individual components of the Rae and Hearne occurred at ∼2.6–2.5 Ga, or later during Paleoproterozoic tectonic events. Further work is needed to understand the internal evolution of the Hearne during the Neoarchean and Paleoproterozoic in order to develop more comprehensive tectonic models.

Acknowledgements

The assistance of the technical staff at the Geochronology lab is gratefully acknowledged. Julie Peressini contributed to final manuscript preparations. Natasha Wodicka provided constructive comments on an early draft of the manuscript. Comments by journal reviewers Pat Bickford and Kevin Ansdell were very beneficial.

References

Aspler, L.B., Armitage, A.E., Ryan, J.J., Hauseux, M., Surmacz, S., Harvey, B.J.A., 2000. Precambrian geology, Victory and Mackenzie Lakes, Nunavut and significance of Mackenzie Lake metasediments, Paleoproterozoic Hurwitz Group. Geological Survey of Canada, Current Research 2000-C10, p. 10.

Aspler, L.B., Chiarenzelli, J.R., 1996. Stratigraphy, sedimentology and physical volcanology of the Henik Group, central Ennadai-Rankin greenstone belt, Northwest Territories Canada: Late Archean paleogeography of the Hearne Province and tectonic implications. Precambrian Res. 77, 59–89.

Aspler, L.B., Chiarenzelli, J.R., Cousens, B.L., Valentino, D., 1999. Precambrian geology, northern Angikuni Lake, and a transect across the Snowbird tectonic zone, western Angikuni Lake, Northwest Territories (Nunavut). Geological Survey of Canada Current Research 1999-C, pp. 107–118.

Berman, R.G., Davis, W.J., Aspler, L.B., Chiarenzelli, J.R., 2002a. SHRIM U–Pb Ages of Multiple Metamorphic Events in the Angikuni Lake area, western Churchill Province, Nunavut. Radiogenic Age and Isotopic Studies: Report 15. Geological Survey of Canada Paper 2002-F3, p. 9.

Berman, R.G., Davis, W.J., Ryan, J.J., Tella, S., Brown, N., 2002b. In situ SHRIM U–Pb Geochronology of Barrovian Facies-Series Metasedimentary Rocks in the Happy Lake and Josephine River supracrustal Belts: Implications for the Paleoproterozoic Architecture of the Northern Hearne Domain, Nunavut. Radiogenic Age and Isotopic Studies: Report 15. Geological Survey of Canada, Current Research 2002-F4, p. 14.

Berman, R., Ryan, J.J., Tella, S., Sanborn-Barrie, M., Stern, R., Aspler, L., Hanmer, S., Davis, W., 2000. The case of multiple metamorphic events in the western Churchill Province: evidence from linked thermobarometric and in-situ SHRIMP data, and jury deliberations. In: Proceedings of Geological Association of Canada Meeting (GeoCanada 2000), May 29–June 2, Calgary, AB, p. 4.

Carson, C.J., Berman, R.G., Stern, R.A., Sanborn-Barrier, M., Skulski, T., Sandeman, H.A.I., 2004. Age constraints on the Paleoproterozoic tectonometamorphic history of the Committee Bay region, western Churchill Province Canada; evidence from zircon and in situ monazite SHRIMP geochronology. Can. J. Earth Sci. 41, 1049–1076.

Cousens, B.L., Aspler, L.B., Chiarenzelli, J.R., 2004. Geochemistry and Sm-Nd isotope composition of Neoarchean supracrustal and plutonic rocks, Henik segment, Central Hearne supracrustal belt, Nunavut Canada. Precambrian Res. 134, 169–188.

Cumming, G.L., Richards, J.R., 1975. Ore lead isotope ratios in a continuously changing Earth. Earth Planet. Sci. Lett. 28, 155.

Davis, W.J., Hanmer, S., Aspler, L., Sandeman, H., Tella, S., Zaleski, E., Relf, C., Ryan, J., Berman, R., MacLachlan, K., 2000. Regional differences in the Neoarchean crustal evolution of the western Churchill Province: can we make sense of it? In: Proceedings of Geological Association of Canada Meeting (GeoCanada 2000), May 29–June 2, Calgary, AB, 4 pp.

Davis, W.J., Hanmer, S., Sandeman, H.A., 2004. Temporal evolution of the Neoarchean Central Hearne supracrustal belt: rapid generation of juvenile crust in a suprasubduction zone setting. Precambrian Res. 134, 85–112.

Davis, W.J., McNicoll, V.J., Bellerive, D.R., Santowski, K., Scott, D.J., 1997. Modified Chemical Procedures for the Extraction and Purification of Uranium from Titanite, Allanite and Rutile in the Geochronology Laboratory, Geological Survey of Canada. Radiogenic Age and Isotopic Studies: Report 10. Geological Survey of Canada Current Research 97-F, pp. 33–35.

Davis, W.J., Zaleski, E., 1998. Geochronological Investigations of the Woodburn Lake group, western Churchill Province, Northwest Territories: Preliminary Results. Current Research, Geological Survey of Canada Paper 98-F, pp. 89–97.

Eade, K.E., 1986. Precambrian geology of the Tulemalu Lake–Yathkyed Lake area, District of Keewatin. Geological Survey of Canada, Paper 84-11, p. 31.

Fahrig, W.F., Christie, K.W., Eade, K.E., Tella, S., 1984. Paleomagnetism of the Tulemalu dykes, northwest territories Canada. Can. J. Earth Sci. 21, 544–553.

Frisch, T., 1982. Precambrian geology of the Prince Albert Hills, western Melville Peninsula, northwest territories. Geological Survey of Canada Bulletin 346, p. 70.

Gibb, R.A., Thomas, M.D., Lapointe, P.L., Mukhopadyay, M., 1983. Geophysics of the proposed Proterozoic sutures in Canada. Precambrian Res. 19, 349–384.

Hanmer, S., Relf, C., 2000. Western Churchill NATMAP Project: new results and potential significance. In: Proceedings of Geological Association of Canada Meeting (GeoCanada 2000), May 29–June 2, Calgary, AB, 4 pp.

Hanmer, S., Sandeman, H.A., Davis, W.J., Aspler, L.B., Rainbird, R.H., Ryan, J.J., Relf, C., Peterson, T.D., 2004. Geology and Neoarchean tectonic setting of the Central Hearne supracrustal belt, western Churchill Province, Nunavut Canada. Precambrian Res. 134, 63–83.

Hanmer, S., Tella, S., Ryan, J.J., Sandeman, H.A., Berman, R.G., 2006. Late Neoarchean thick-skinned thrusting and Paleoproterozoic reworking in the MacQuoid supracrustal belt and Cross Bay plutonic complex, western Churchill Province, Nunavut, Canada. Precambrian Res. 144 (1–2), 126–139.

Hanmer, S., Tella, S., Sandeman, H.A., Ryan, J.J., Hadlari, T., Mills, A., 1999a. Proterozoic reworking in western Churchill Province, Gibson Lake–Cross Bay area, northwest territories (Kivalliq region, Nunavut). Part I: general geology. Current Research, Geological Survey of Canada Paper 99-C, pp. 55–64.

Hanmer, S., Tella, S., Sandeman, H.A., Ryan, J.J., Hadlari, T., Mills, A., 1999b. Proterozoic reworking in western Churchill Province, Gibson Lake–Cross Bay area, northwest territories (Kivalliq region, Nunavut). Part II: regional structural geology. Current Research, Geological Survey of Canada Paper 99-C, pp. 65–75.

Hanmer, S., Williams, M., Kopf, C., 1995. Striding-Athabasca mylonite zone: implications for Archean and Proterozoic tectonics of the western Canadian shield. Can. J. Earth Sci. 32, 178–196.

Henderson, J.R., Henderson, M.N., Pryer, L.L., Cresswell, R.G., 1991. Geology of the Whitehills-Tehek area, District of Keewatin: an Archean supracrustal belt with iron-formation-hosted gold mineralization in the central Churchill Province. Current Research, Geological Survey of Canada Paper 91-C, pp. 149–156.

Hoffman, P.F., 1988. United plates of America, the birth of a craton: early Proterozoic assembly and growth of Laurentia. Ann. Rev. Earth Planet. Sci. 16, 543–603.

Krogh, T.E., 1982. Improved accuracy of U–Pb ages by the creation of more concordant systems using an air abrasion technique. Geochim. Cosmochim. Acta 46, 637–649.

LeCheminant, A.N., Roddick, J.C., 1991. U–Pb Zircon Evidence for Widespread 2.6 Ga Felsic Magmatism in the Central District of Keewatin, N.W.T. Radiogenic Age and Isotopic Studies: Report 4. Geological Survey of Canada 90-2, pp. 91–99.

LeCheminant, A.N., Tella, S., Sanborn-Barrie, M., Venance, K.E., 1997. Geology, Parker Lake South, District of Keewatin, Northwest Territories. Geological Survey of Canada, Open File Map 3405, scale 1:50,000.

Ludwig, K.R., 2001. User's Manual for Isoplot/Ex, Rev. 2.49: A Geochronological Toolkit for Microsoft Excel. Special Publication, 1a, Berkeley Geochronology Center, Berkeley, 55 pp.

MacLachlan, K., Davis, W.J., Relf, C., 2005a. U/Pb geochronological constraints on Neoarchean tectonism: multiple compressional events in the northwestern Hearne Domain, western Churchill Province Canada. Can. J. Earth Sci. 42, 85–109.

MacLachlan, K., Davis, W.J., Relf, C., 2005b. Paleoproterozoic reworking of an Archean thrust fault in the Hearne domain western Churchill Province: U–Pb geochronological constraints. Can. J. Earth Sci. 42, 1313–1330.

MacLachlan, K., Relf, C., 2000. Regional Geological Compilation Map of the Yathkyed Greenstone Belt (parts of NTS 65G/9, 15 and 16, 65H/13, 65I/3–7, 10, 11, 14, 15 and 65J/1) western Churchill Province, Nunavut, Northwest Territories Geology Division. Department of Indian Affairs and Northern Development, EGS Open File 2000-01, scale 1:125,000.

MacLachlan, K., Relf, C., Davis, W.J., 2000. U–Pb geochronological constraints on structures controlling distribution of tectonothermal domains, Yathkyed–Angikuni area, western Churchill Province. In: Proceedings of Geological Association of Canada Meeting (GeoCanada 2000), May 29–June 2, Calgary, AB, 4 pp.

Mahan, K.H., Williams, M.L., Baldwin, J.A., 2003. Contractional uplift of deep crustal rocks along the Legs Lake shear zone, western Churchill Province Canadian Shield. Can. J. Earth Sci. 40, 1085–1110.

Mills, A., Berman, R., Hanmer, S., Davis, W., 2000. New insights into the tectonometamorphic history of the Uvauk complex, Nunavut. In: Proceedings of Geological Association of Canada Meeting (GeoCanada 2000), May 29–June 2, 2000, Calgary, AB, 4 pp.

Parrish, R.R., Roddick, J.C., Loveridge, W.D., Sullivan, R.W., 1987. Uranium–Lead Analytical Techniques at the Geochronology Laboratory, Geological Survey of Canada. Radiogenic Age and Isotopic Studies: Report 1. Geological Survey of Canada, Paper 87-2, pp. 3–7.

Peterson, T.D., van Breemen, O., Sandeman, H.A., Cousens, B.L., 2002. Proterozoic (1.85–1.75 Ga) igneous suites of the western Churchill Province: granitoid and ultrapotassic magmatism in a reworked Archean hinterland. Precambrian Res. 119, 73–100.

Peterson, T.D., van Breemen, O., Sandeman, H.A., Rainbird, R.H., 2000. Proterozoic (1.85–1.75 Ga) granitoid plutonism and tectonics of the western Churchill Province. In: Proceedings of Geological Association of Canada Meeting (GeoCanada 2000), May 29–June 2, Calgary, AB, 4 pp.

Rainbird, R.H., Hadlari, T., Aspler, L.B., Donaldson, J.A., LeCheminant, A.N., Peterson, T.D., 2003. Sequence stratigraphy and evolution of the Paleoproterozoic intracontinental Baker Lake and Thelon basins, western Churchill Province, Nunavut Canada. Precambrian Res. 125, 21–53.

Roddick, J.C., 1987. Generalized numerical error analysis with applications to geochronology and thermodynamics. Geochim. Cosmochim. Acta 51, 2129–2135.

Roddick, J.C., Henderson, J.R., Chapman, H.J., 1992. U–Pb ages from Archean Whitehills-Tehek lakes supracrustal belt, Churchill Province, District of Keewatin, Northwest Territories. Radiogenic Age and Isotopic Studies: Report 6. Geological Survey of Canada Paper 92-2, pp. 31–40.

Roddick, J.C., Loveridge, W.D., Parrish, R.R., 1987. Precise U–Pb dating of zircon at the sub-nanogram Pb level. Chem. Geol. 66, 111–121.

Romer, R.L., 2001. Lead incorporation during crystal growth and the misinterpretation of geochronological data from low-238U/204Pb metamorphic mineral. Terra Nova 13, 258–263.

Ross, G.M., 2002. Evolution of Precambrian continental lithosphere in western Canada: results from Lithoprobe studies in Alberta and beyond. Can. J. Earth Sci. 39, 413–437.

Ryan, J.J., Davis, W., Berman, R., Hanmer, S., Tella, S., Sandeman, H., 2000. Regional foliation development in the MacQuoid Lake–Gibson Lake–Akunak Bay area (western Churchill Province): looking through Paleoproterozoic reworking at a Neoarchean orogenic event. In: Proceedings of Geological Association of Canada Meeting (GeoCanada 2000), May 29–June 2, Calgary, AB, 4 pp.

Ryan, J.J., Hanmer, S., Tella, S., Sandeman, H.A., 1999. Detailed structural studies, Gibson Lake–Cross Bay–MacQuoid Lake area, northwest territories (Kivalliq Region, Nunavut). Current Research, Geological Survey of Canada Paper 99-C, pp. 87–96.

Sanborn-Barrie, M., 1999. Geology, geothermobarometry and geochronology of the Paleoproterozoic high-P granulite-facies Kramanituar Complex, western Churchill Province. Ph.D. Thesis. Carleton University, p. 258.

Sanborn-Barrie, M., Carr, S.D., Theriault, R., 2001. Geochronological constraints on metamorphism, magmatism and exhumation of deep-crustal rocks of the Kramanituar Complex, with implications for the Paleoproterozoic evolution of the Archean western Churchill Province Canada. Contrib. Mineral. Petrol. 141, 592–612.

Sandeman, H.A., Davis, W.J., Hanmer, S., MacLachlan, K., Ryan, J.J., Kjarsgaard, B., Kerswill, J., Tella, S., Zaleski, E., Cousens, B., Relf, C., 2000a. Archean volcanic sequences of the western Churchill Province, Nunavut, Canada: three petrochemically distinct domains of non-plateau affinity. In: Proceedings of Geological Association of Canada Meeting (GeoCanada 2000), May 29–June 2, Calgary, AB, 4 pp.

Sandeman, H.A., Lepage, L.D., Ryan, J.J., Tella, S., 2000b. Field evidence for commingling between ca. 1830 Ma lamprophyre, monzonitic, and monozogranitic magmas, MacQuoid–Gibson lakes area, Nunavut. Current Research, Geological Survey of Canada 2000-C5, pp. 1–9.

Sandeman, H.A., Davis, W.J., Hanmer, S., Tella, S., Ryan, J.J., 2006. Tectonic evolution of the northwestern Hearne domain, western Churchill Province, Canada: a petrochemical perspective from the MacQuoid supracrustal belt. Precambrian Res. 144 (1–2), 140–165.

Sandeman, H.A., Hanmer, S., Davis, W.J., Ryan, J.J., Peterson, T.D., 2004a. Whole-rock and Nd isotopic geochemistry of Neoarchean granitoids and their bearing on the evolution of the Central Hearne supracrustal belt, western Churchill Province Canada. Precambrian Res. 134, 143–167.

Sandeman, H.A., Hanmer, S., Peterson, T.D., Davis, W.J., Ryan, J.J., 2004b. Neoarchean volcanic rocks, Central Hearne supracrustal belt, western Churchill Province Canada: geochemical and isotopic evidence supporting intraoceanic suprasubduction zone extension. Precambrian Res. 134, 113–141.

Schau, M., Fraser, J.A., Heywood, W.W., 1978. Metamorphism of the Prince Albert Group, District of Keewatin. Geological Survey of Canada Paper 78-10, pp. 203–213.

Skulski, T., Sandeman, H., Sanborn-Barrie, M., MacHattie, T., Young, M., Carson, C., Berman, R., Brown, J., Rayner, N., Panagapko, D., Byrne, D., Deyell, C., 2003. Bedrock Geology of the Ellice Hills map area and new constraints on the regional geology of the Committee Bay area, Nunavut. Geological Survey of Canada, Current Research 2003-C22, 14 pp.

Stern, R.A., 1997. The GSC Sensitive High Resolution Ion Microprobe (SHRIMP): Analytical Techniques of Zircon U–Th–Pb Age Determinations and Performance Evaluation. Radiogenic Age and Isotopic Studies, Report 10. Geological Survey of Canada, Current Research 1997-F, pp. 1–31.

Stern, R.A., Amelin, Y., 2003. Assessment of errors in SIMS zircon U–Pb geochronology using a natural zircon standard and NIST SRM 610 glass. Chem. Geol. 197, 111–146.

Stern, R.A., Berman, R.G., 2001. Monazite U–Pb and Th–Pb geochronology by ion microprobe, with an application to in situ dating of an Archean metasedimentary rock. Chem. Geol. 172, 113–130.

Tella, S., Hanmer, S., Sandeman, H.A., Ryan, J.J., Mills, A., Davis, W.J., Berman, R.G., Wilkinson, L., Kerswill, J.A., 2001. Geology, MacQuoid Lake–Gibson Lake–Cross Bay–Akunak Bay region, western Churchill Province, Nunavut. Geological Survey of Canada Map 2008A, scale 1:100,000.

Tella, S., Heywood, W.W., Loveridge, W.D., 1985. A U–Pb Age on Zircon from a Dacite Porphyry, Amer Lake Map Area, District of Keewatin, NWT. Current Research, Geological Survey of Canada Paper 85-1B, pp. 371–374.

Tella, S., LeCheminant, A.N., Sanborn-Barrie, M., Venance, K.E., 1997a. Geology and Structure of Parts of the MacQuoid Lake area, District of Keewatin, Northwest Territories. Current Research, Geological Survey of Canada Paper 1997-C, pp. 123–132.

Tella, S., LeCheminant, A.N., Sanborn-Barrie, M., Venance, K.E., 1997b. Geology, parts of MacQuoid Lake, District of Keewatin, Northwest Territories. Geological Survey of Canada, Open File Map 3404, scale 1:50.000.

Tella, S., Roddick, J.C., 1995. U–Pb Zircon Age for a Volcanic Suite in the Rankin Inlet Group, Rankin Inlet map area, District of Keewatin, Northwest Territories. Radiogenic Age and Isotopic Studies: Report 9. Geological Survey of Canada Paper 1995-F, pp. 11–15.

Tella, S., Ryan, J.J., Sandeman, H.A., Hanmer, S., Mills, A., Wilkinson, L., 2000. Proterozoic Reworking in a Portion of the western Churchill Province, Akunak Bay Area, Nunavut. Current Research, Geological Survey of Canada Paper 2000-C11, pp. 1–9.

Thomas, M.D., Gibb, R.A., 1985. Proterozoic plate subduction and collision: processes for reactivation of Archean crust in the Churchill Province. Geological Association of Canada, Special Paper 28, pp. 264–279.

van Breemen, O., Peterson, T.D., Sandeman, H.A., 2005. U–Pb zircon geochronology and Nd isotope geochemistry of Proterozoic granitoids in the western Churchill Province: intrusive age pattern and Archean source domains. Can. J. Earth Sci. 42, 339–377.

van Staal, C., Dewey, J.F., Mac-Niocaill, C., McKerrow, W.S., 1998. The Cambrian-Silurian tectonic evolution of the Northern Appalachians and British Caledonides; history of a complex, west and southwest Pacific-type segment of Iapetus. In: Blundell, D.J., Scott, A.C. (Eds.), Lyell; The Past is the Key to the Present, vol. 143. Geological Society Special Publications, pp. 199–242.

York, D., 1969. Least squares fitting of a straight line with correlated errors. Earth Planet. Sci. Lett. 5, 320–324.

Zaleski, E., Davis, W.J., Sandeman, H.A., 2001. Continental rifting, mantle magmas and basement/cover relationships. 4th International Archean Symposium, Perth, Australia, pp. 374–376 (Programme with Abstracts 4).